

# Introduction to Computational Neuroscience

Biol 698

Math 635

Biol 498

Math 430

## Bibliography:

"Mathematical Foundations of Neuroscience", by G. B. Ermentrout & D. H. Terman - Springer (2010), 1st edition. ISBN 978-0-387-87707-5

\* "Dynamical Systems in Neuroscience: The Geometry of Excitability and Bursting", by Eugene M. Izhikevich. The MIT Press, 2007. ISBN 0-262-09043-8

# Overview

## Two-dimensional models

- Reduction of the Hodgkin-Huxley model to two-dimensional models (review)
- Two-dimensional neural models
- Two-dimensional dynamical systems
- Phase portraits and vector fields
- Equilibria and stability
- Bifurcations

# Two-dimensional neural models

$$\begin{aligned}
 C \dot{V} &= I - \overbrace{\bar{g}_K n^4 (V - E_K)}^{I_K} - \overbrace{\bar{g}_{Na} m^3 h (V - E_{Na})}^{I_{Na}} - \overbrace{g_L (V - E_L)}^{I_L} \\
 \dot{n} &= (n_\infty(V) - n) / \tau_n(V), \\
 \dot{m} &= (m_\infty(V) - m) / \tau_m(V), \\
 \dot{h} &= (h_\infty(V) - h) / \tau_h(V),
 \end{aligned}$$

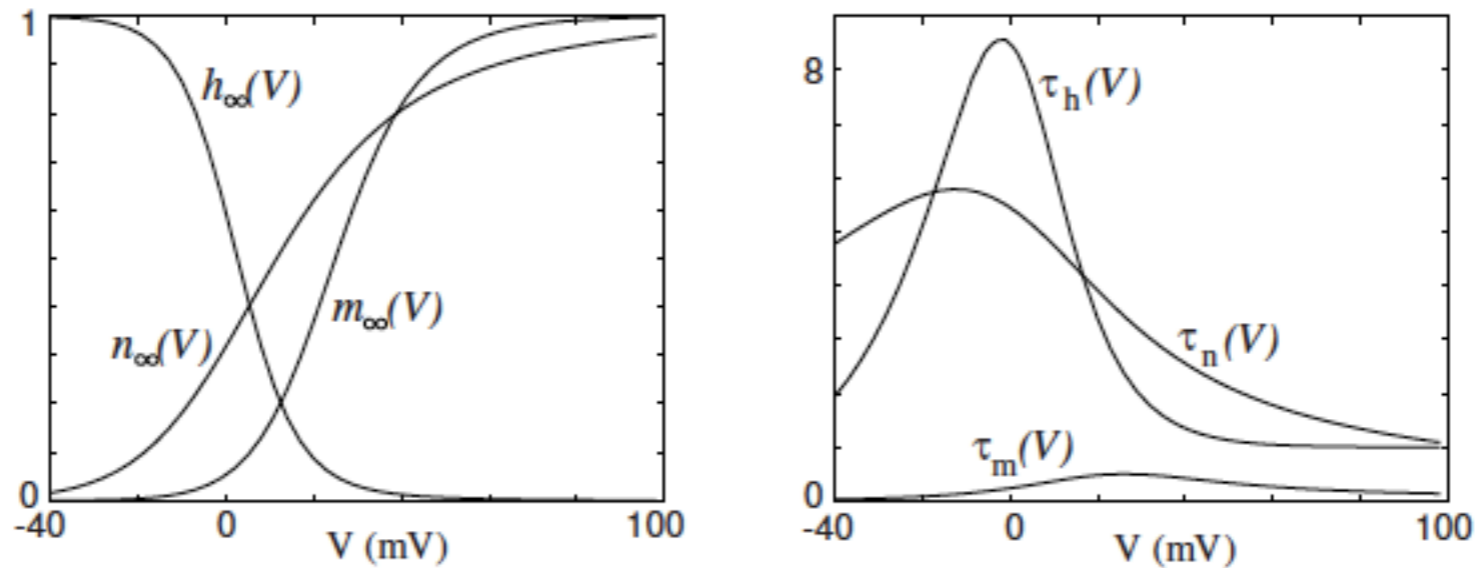


Figure 2.13: Steady-state (in)activation functions (left) and voltage-dependent time constants (right) in the Hodgkin-Huxley model.

# Two-dimensional neural models

$$C\dot{V} = I - \overbrace{\bar{g}_K n^4 (V - E_K)}^{I_K} - \overbrace{\bar{g}_{Na} m^3 \cancel{h} (V - E_{Na})}^{I_{Na}} - \overbrace{g_L (V - E_L)}^{I_L}$$

$$\dot{n} = (n_\infty(V) - n) / \tau_n(V),$$

$$\dot{m} = (m_\infty(V) - m) / \tau_m(V),$$
~~$$\dot{h} = (h_\infty(V) - h) / \tau_h(V),$$~~

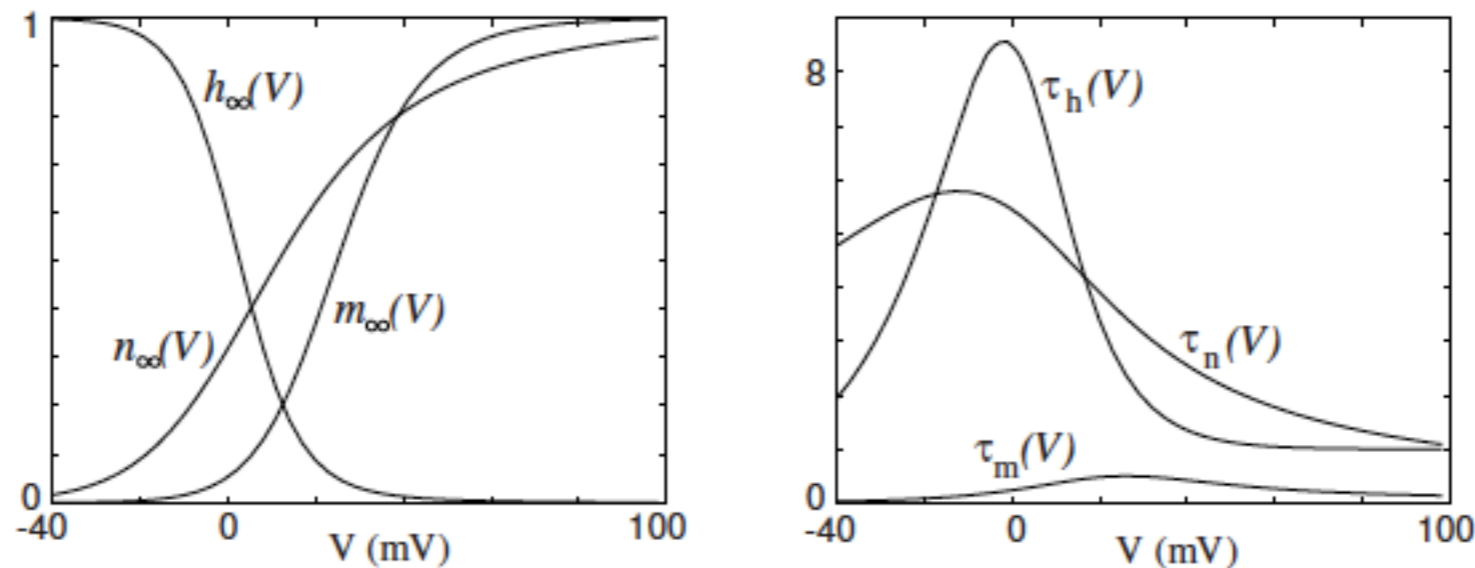


Figure 2.13: Steady-state (in)activation functions (left) and voltage-dependent time constants (right) in the Hodgkin-Huxley model.

# Two-dimensional neural models

$$C\dot{V} = I - \overbrace{\bar{g}_K n^4 (V - E_K)}^{I_K} - \overbrace{\bar{g}_{Na} m^3 h (V - E_{Na})}^{I_{Na}} - \overbrace{g_L (V - E_L)}^{I_L}$$

$$\dot{n} = (n_\infty(V) - n) / \tau_n(V),$$

$$\dot{m} = (m_\infty(V) - m) / \tau_m(V),$$
~~$$\dot{h} = (h_\infty(V) - h) / \tau_h(V),$$~~

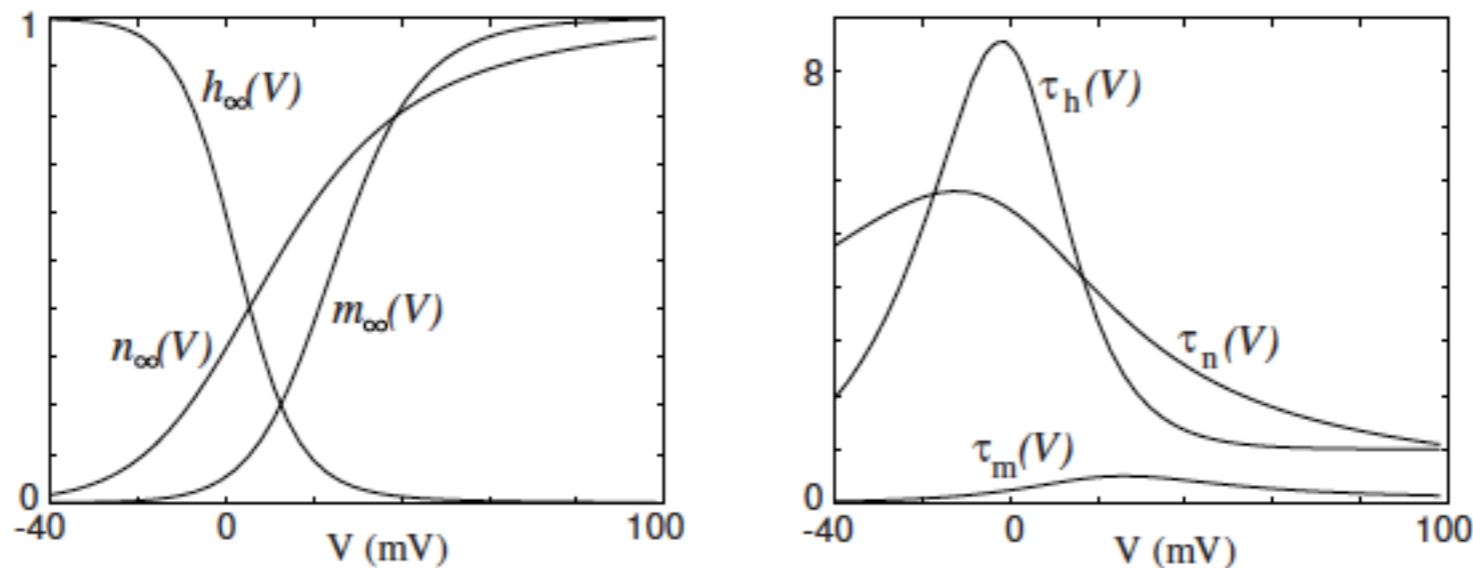


Figure 2.13: Steady-state (in)activation functions (left) and voltage-dependent time constants (right) in the Hodgkin-Huxley model.

# Two-dimensional neural models

- Persistent sodium & potassium model

$$C \frac{dV}{dt} = - G_{Na} m_{\infty}^3(V) (V - E_{Na}) - G_K n^4 (V - E_K) - G_L (V - E_L) + I_{app}$$

$$\frac{dn}{dt} = \frac{n_{\infty}(V) - n}{\tau_n(V)}$$

# Two-dimensional neural models

- Persistent sodium & potassium model

$$C \frac{dV}{dt} = - G_{Na} p_{\infty}^3(V) (V - E_{Na}) - G_K n^4 (V - E_K) - G_L (V - E_L) + I_{app}$$

$$\frac{dn}{dt} = \frac{n_{\infty}(V) - n}{\tau_n(V)}$$



# Two-dimensional neural models

- Morris-Lecar model

$$C \frac{dV}{dt} = - G_{Ca} m_{\infty}(V) (V - E_{Ca}) - G_K w (V - E_K) - G_L (V - E_L) + I_{app}$$

$$\frac{dw}{dt} = \frac{w_{\infty}(V) - w}{\tau_w(V)}$$

# Two-dimensional neural models

- Morris-Lecar model

$$m_{\infty}(V) = 0.5 \left( 1 + \tanh \frac{V + 1}{15} \right)$$

$$w_{\infty}(V) = 0.5 \left( 1 + \tanh \frac{V}{30} \right)$$

$$\tau_w(V) = \frac{5}{\cosh(V / 60)}$$

# Two-dimensional neural model

- FitzHugh-Nagumo (FHN) model

$$\frac{dV}{dt} = V - \frac{V^3}{3} - W + I$$

$$\frac{dW}{dt} = \phi (V + a - bW)$$

$a, b, \phi$ : dimensionless & positive

$\phi \ll 1$ : inverse of a time constant

# Two-dimensional neural models

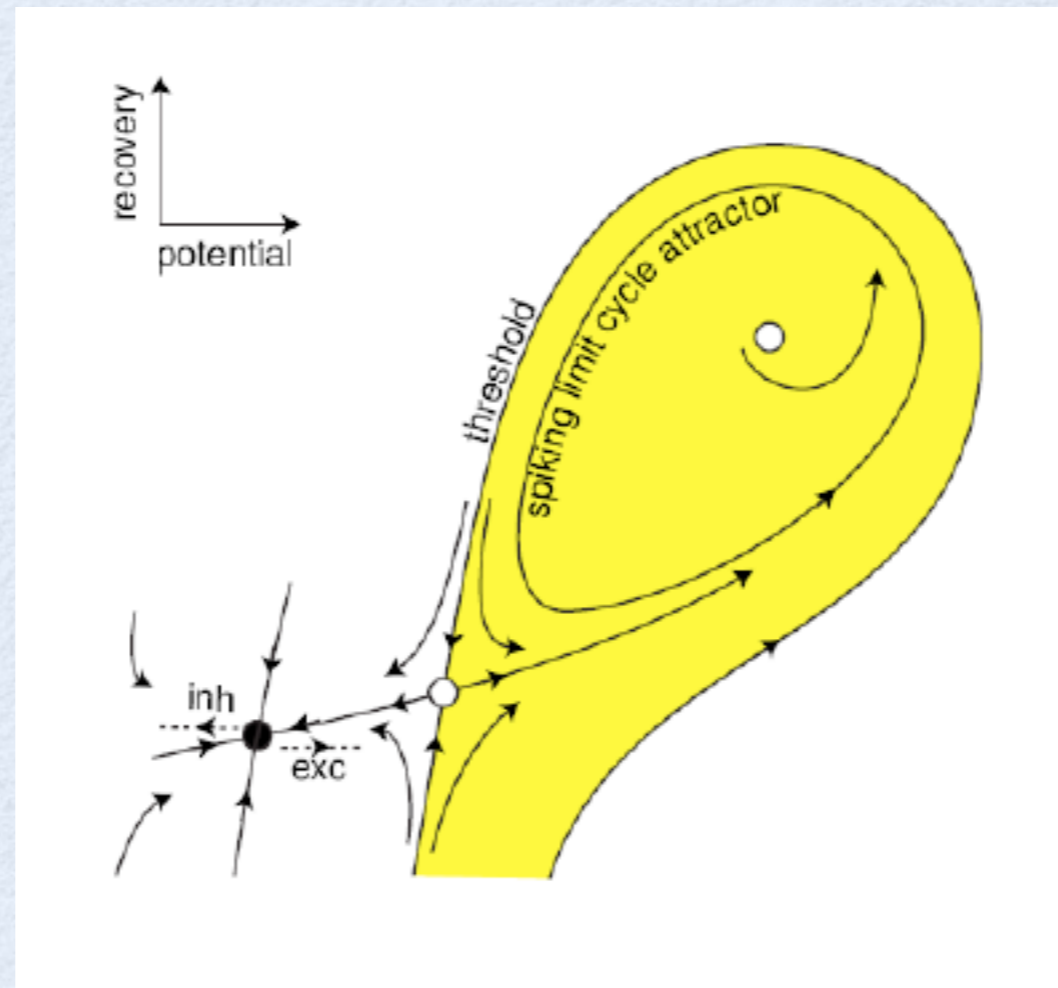
- Quadratic integrate-and-fire model

$$\frac{dV}{dt} = I + V^2 \quad \text{if } V \geq V_{peak}, \text{ then } V \leftarrow V_{reset}$$

$$\text{Equilibria: } V_{rest} = -\sqrt{I} \quad \text{and} \quad V_{thresh} = +\sqrt{I}$$

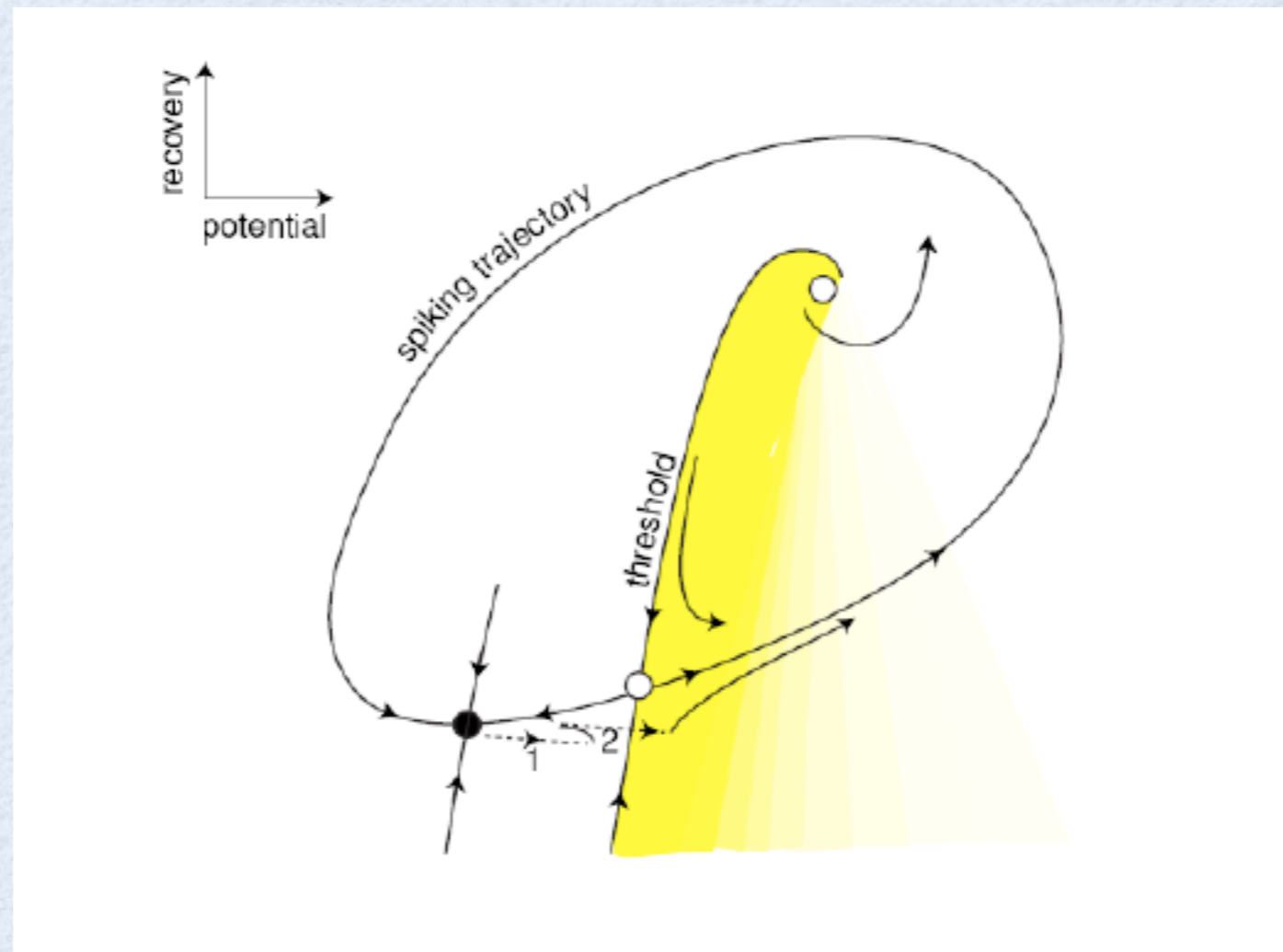
# Bifurcations

- Saddle-node



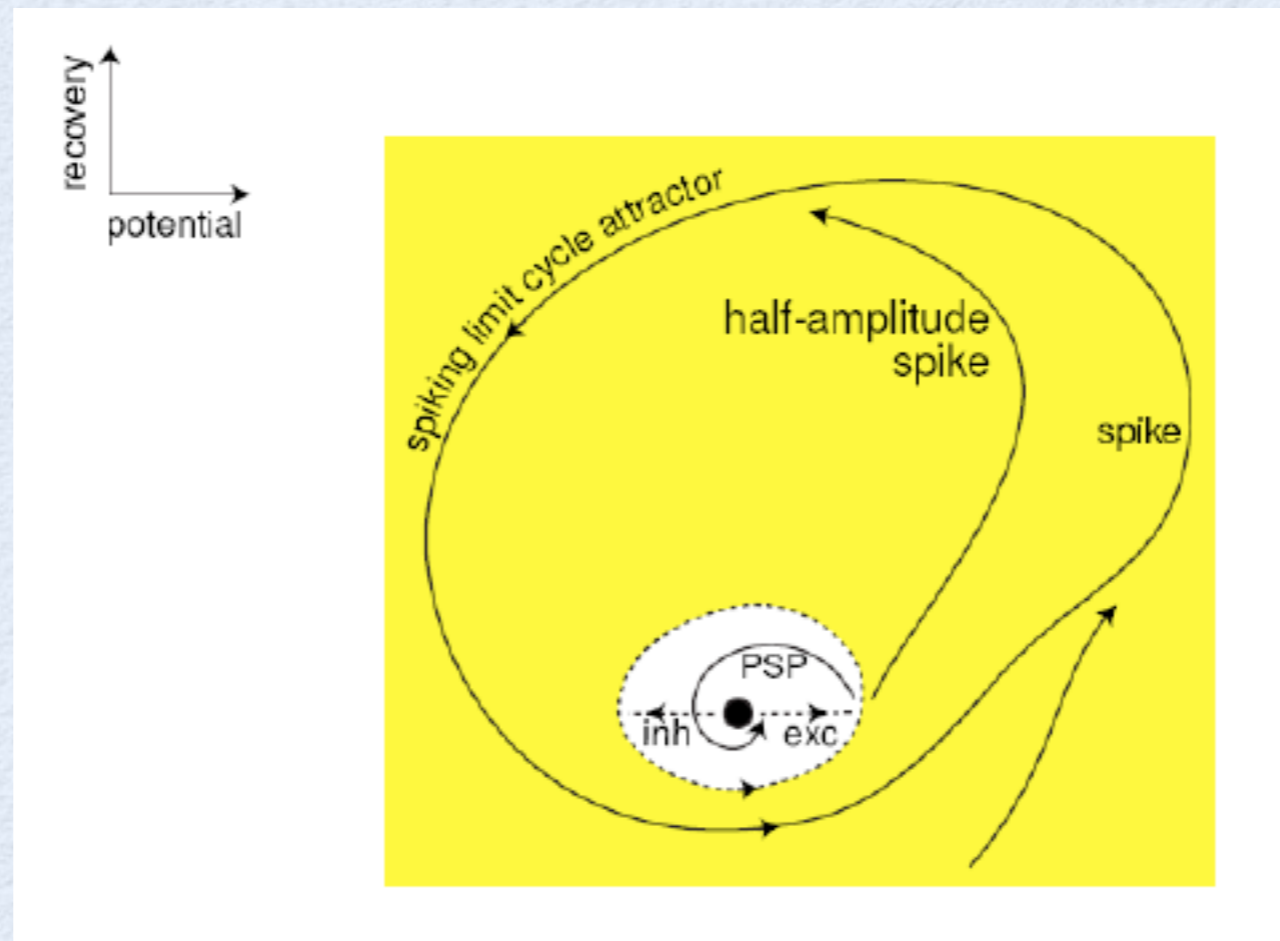
# Bifurcations

- Saddle-node on an invariant circle (SNIC)



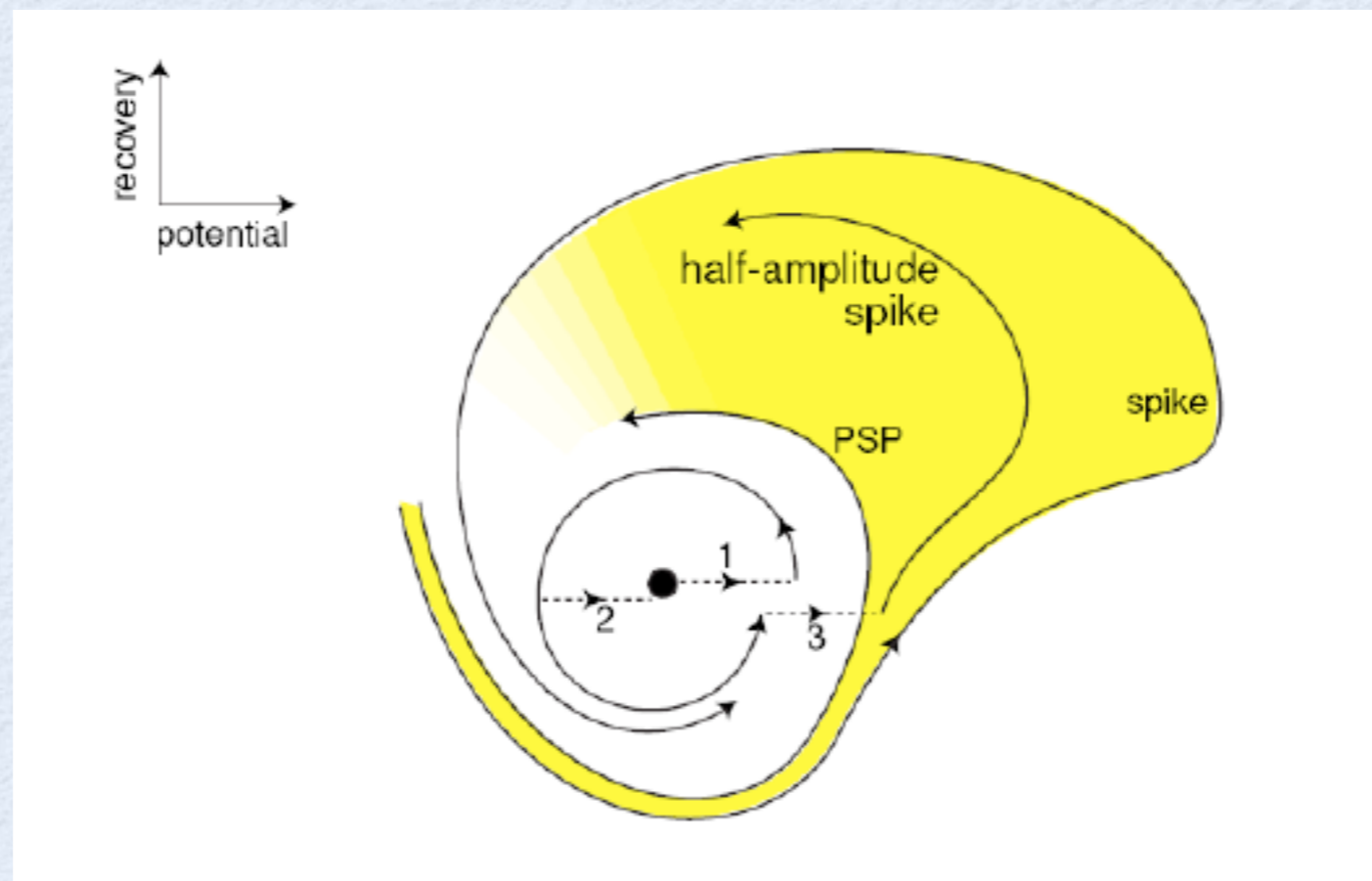
# Bifurcations

- Subcritical Hopf (Andronov-Hopf)



# Bifurcations

- Supercritical Hopf (Andronov-Hopf)



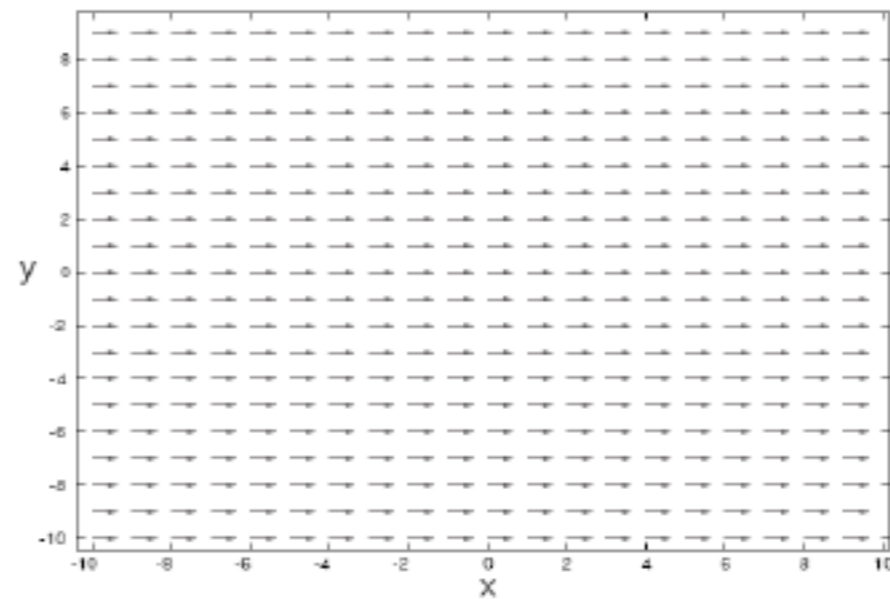


# Two-dimensional dynamical systems

$$\begin{aligned}\frac{dx}{dt} &= f(x, y) & x(0) &= x_0 \\ \frac{dy}{dt} &= g(x, y) & y(0) &= y_0\end{aligned}$$

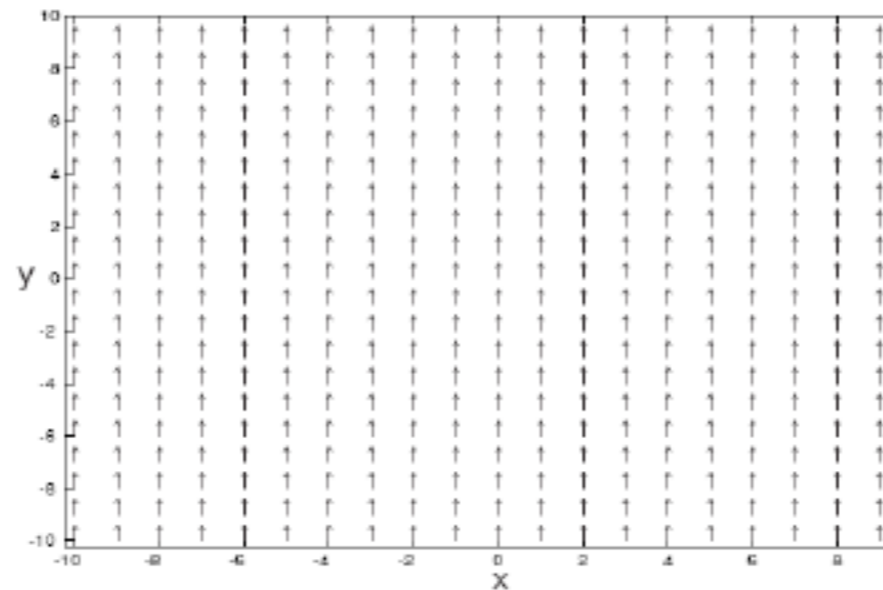
# Two-dimensional dynamical systems

$$\frac{dx}{dt} = 1, \quad \frac{dy}{dt} = 0$$



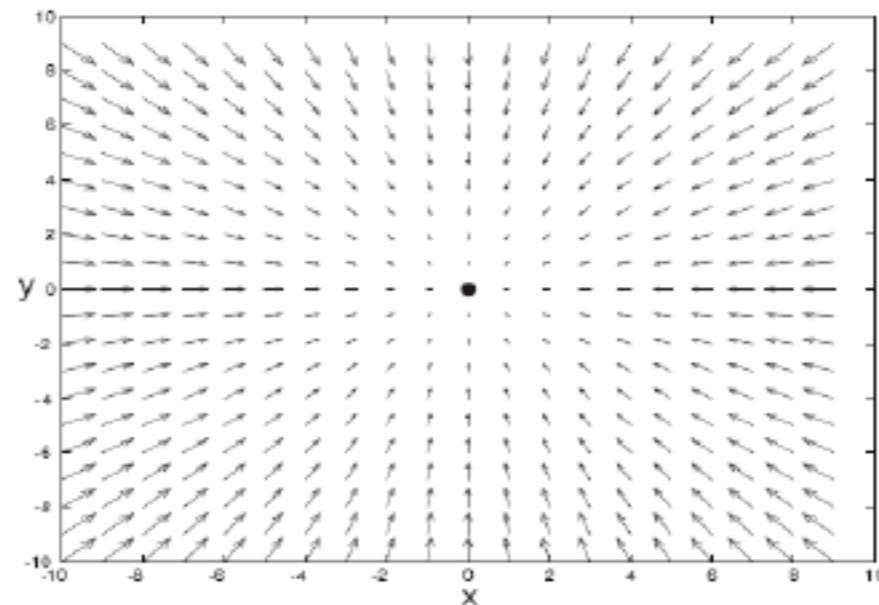
# Two-dimensional dynamical systems

$$\frac{dx}{dt} = 0, \quad \frac{dy}{dt} = 1$$



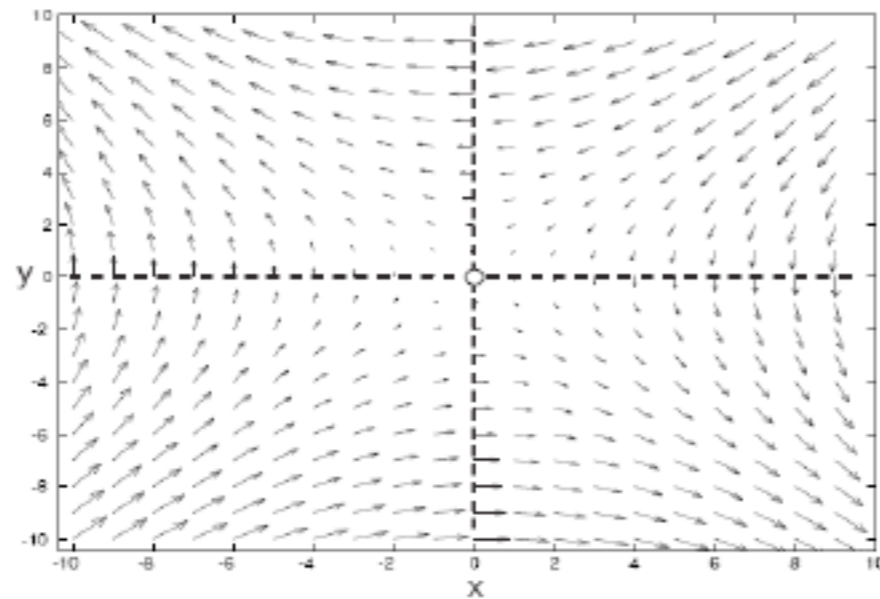
# Two-dimensional dynamical systems

$$\frac{dx}{dt} = -x, \quad \frac{dy}{dt} = -y$$



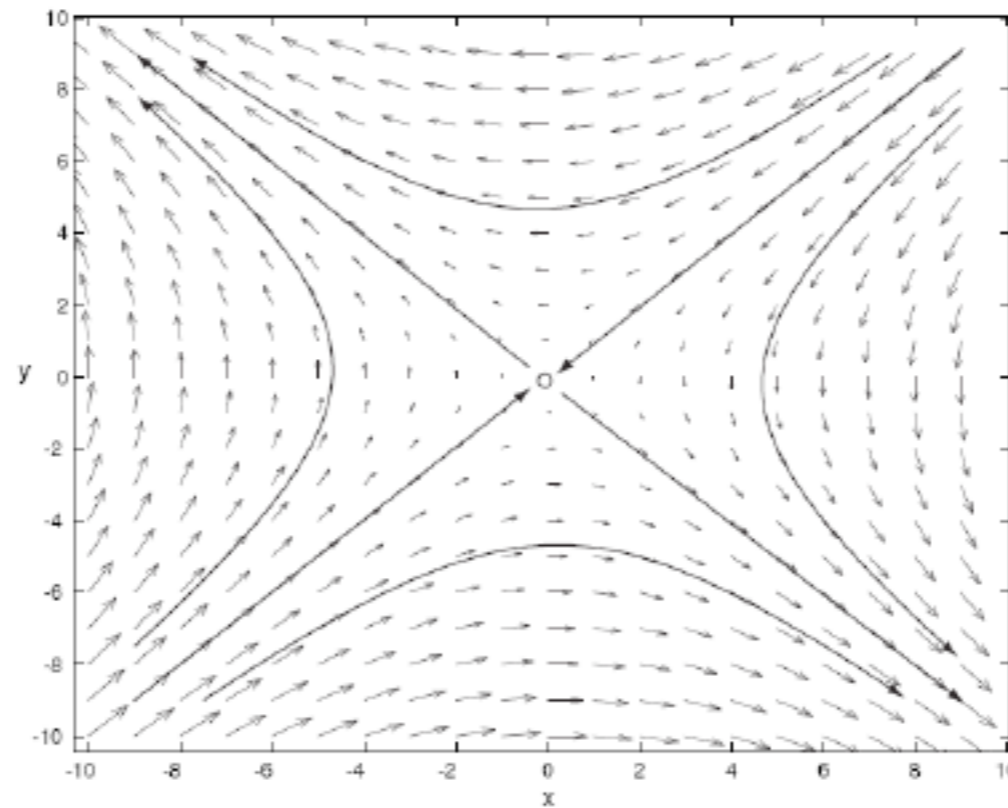
# Two-dimensional dynamical systems

$$\frac{dx}{dt} = -y, \quad \frac{dy}{dt} = -x$$



# Two-dimensional dynamical systems

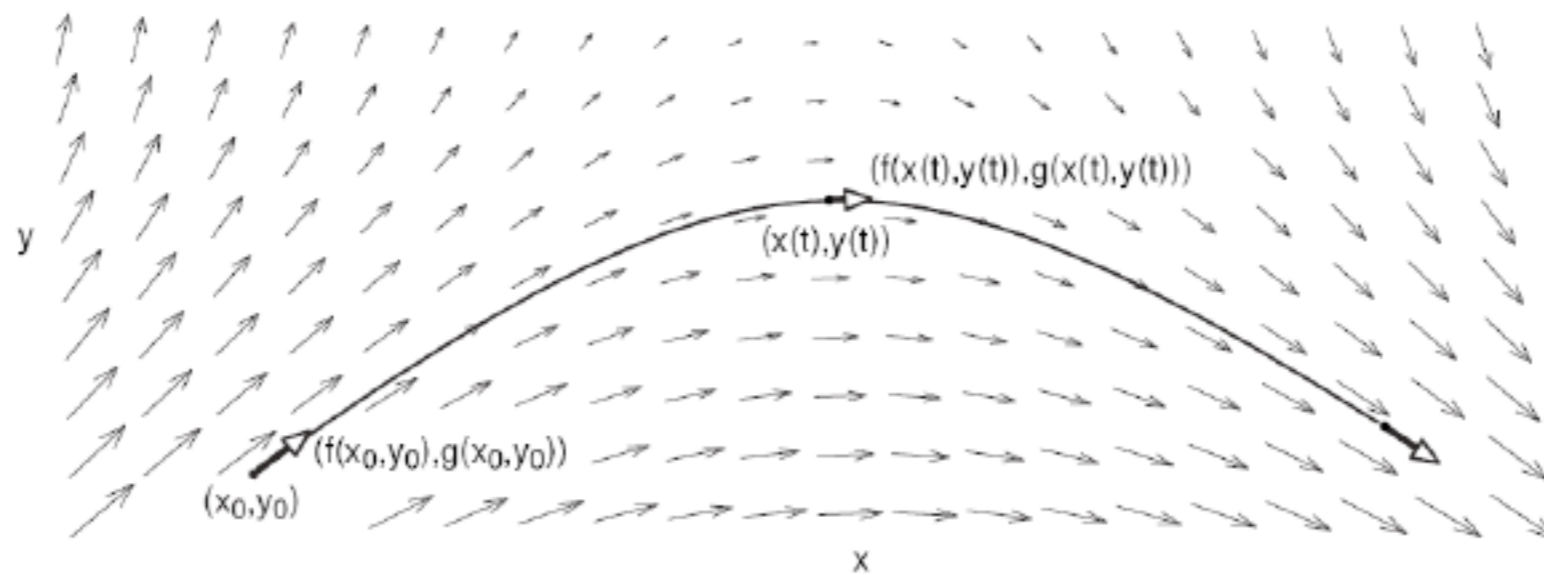
$$\frac{dx}{dt} = -y, \quad \frac{dy}{dt} = -x$$



Solutions are trajectories tangent to the vector field

# Two-dimensional dynamical systems

$$\frac{dx}{dt} = f(x, y), \quad \frac{dy}{dt} = g(x, y)$$



Solutions are trajectories tangent to the vector field

# Two-dimensional dynamical systems

## Limit cycles

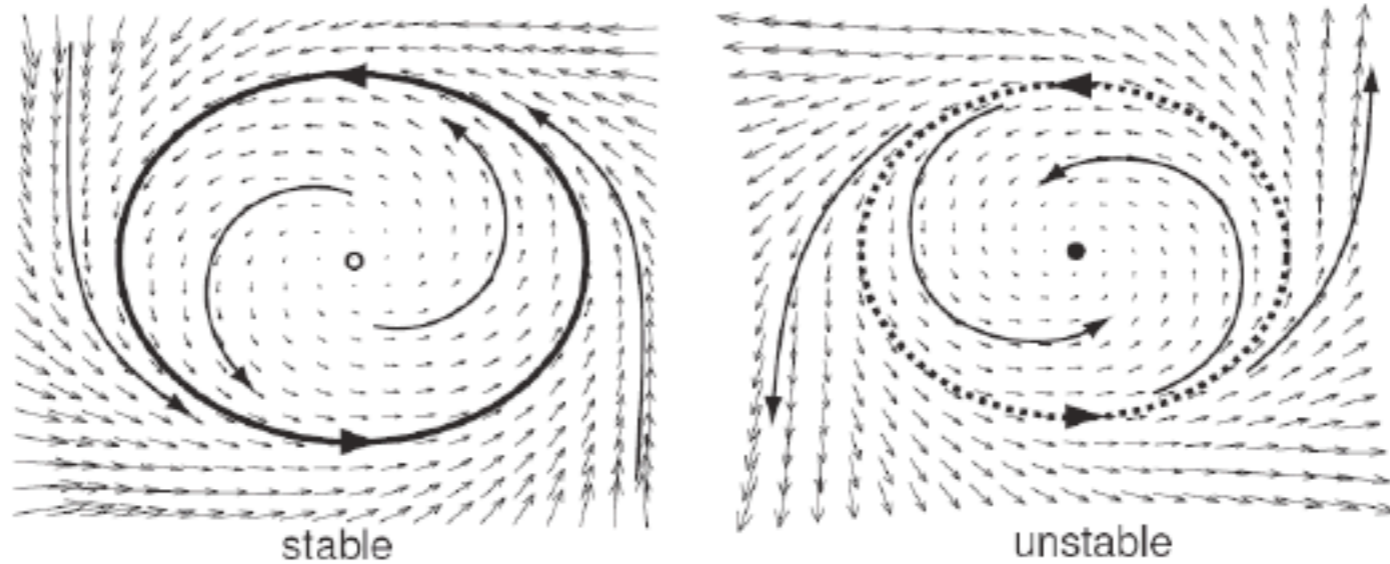
$$\begin{aligned}\frac{dx}{dt} &= f(x, y) & \frac{dy}{dt} &= g(x, y) \\ x(t) &= x(t + T) & y(t) &= y(t + T)\end{aligned}$$

- The minimal value of **T** for which the equality holds is called the **period**



# Two-dimensional dynamical systems

## Limit cycles



- The minimal value of  $T$  for which the equality holds is called the period

# Two-dimensional neural models

□  $I_{Na,p} + I_K$  model

$$C \frac{dV}{dt} = - G_{Na} m_{\infty}(V) (V - E_{Na}) - G_K n (V - E_K) - G_L (V - E_L) + I$$

$$\frac{dn}{dt} = \frac{n_{\infty}(V) - n}{\tau_n(V)}$$

# Two-dimensional neural models

## □ $I_{Na,p} + I_K$ model

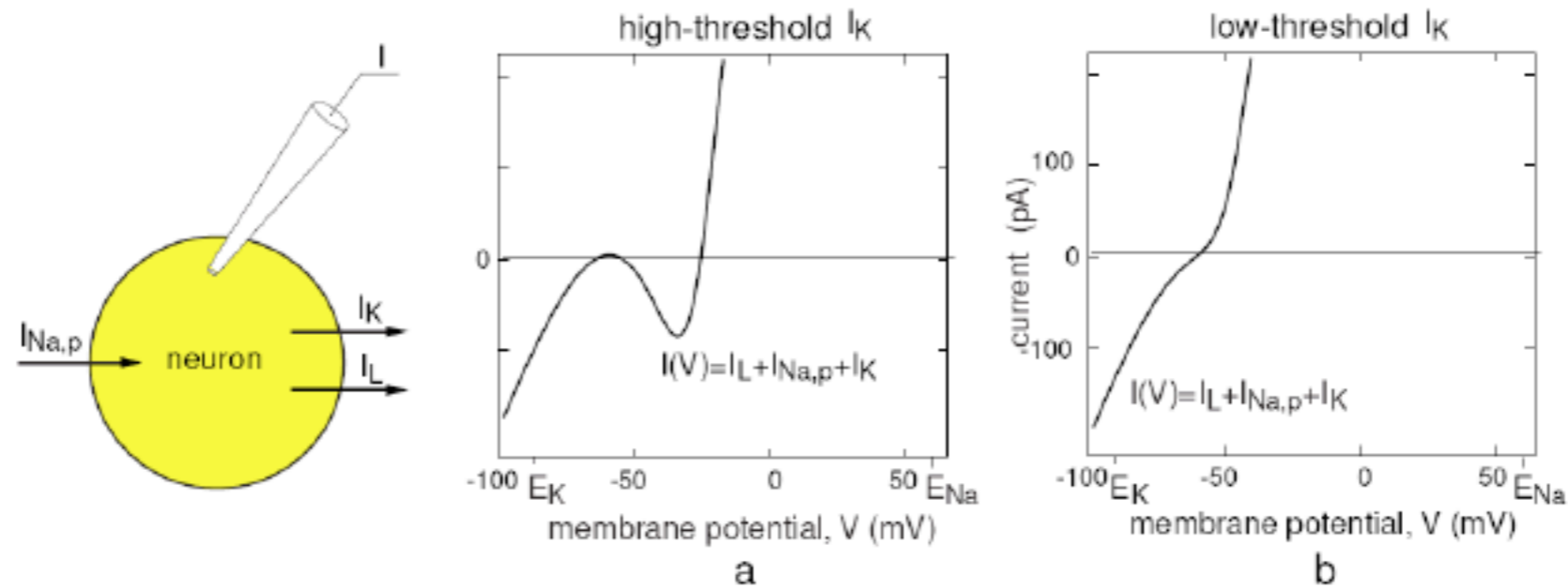


Figure 4.1: The  $I_{Na,p} + I_K$ -model (4.1, 4.2). Parameters in (a):  $C = 1$ ,  $I = 0$ ,  $E_L = -80$  mV,  $g_L = 8$ ,  $g_{Na} = 20$ ,  $g_K = 10$ ,  $m_\infty(V)$  has  $V_{1/2} = -20$  and  $k = 15$ ,  $n_\infty(V)$  has  $V_{1/2} = -25$  and  $k = 5$ , and  $\tau(V) = 1$ ,  $E_{Na} = 60$  mV and  $E_K = -90$  mV. Parameters in (b) as in (a) except  $E_L = -78$  mV and  $n_\infty(V)$  has  $V_{1/2} = -45$ ; see Sect. 2.3.5.

# Two-dimensional neural models

## □ Nullclines

$$n = \frac{I - G_L (V - E_L) - G_{Na} m_\infty(V) (V - E_{Na})}{G_K (V - E_K)}$$

$$n = n_\infty(V)$$

# Two-dimensional neural models

## Phase-plane

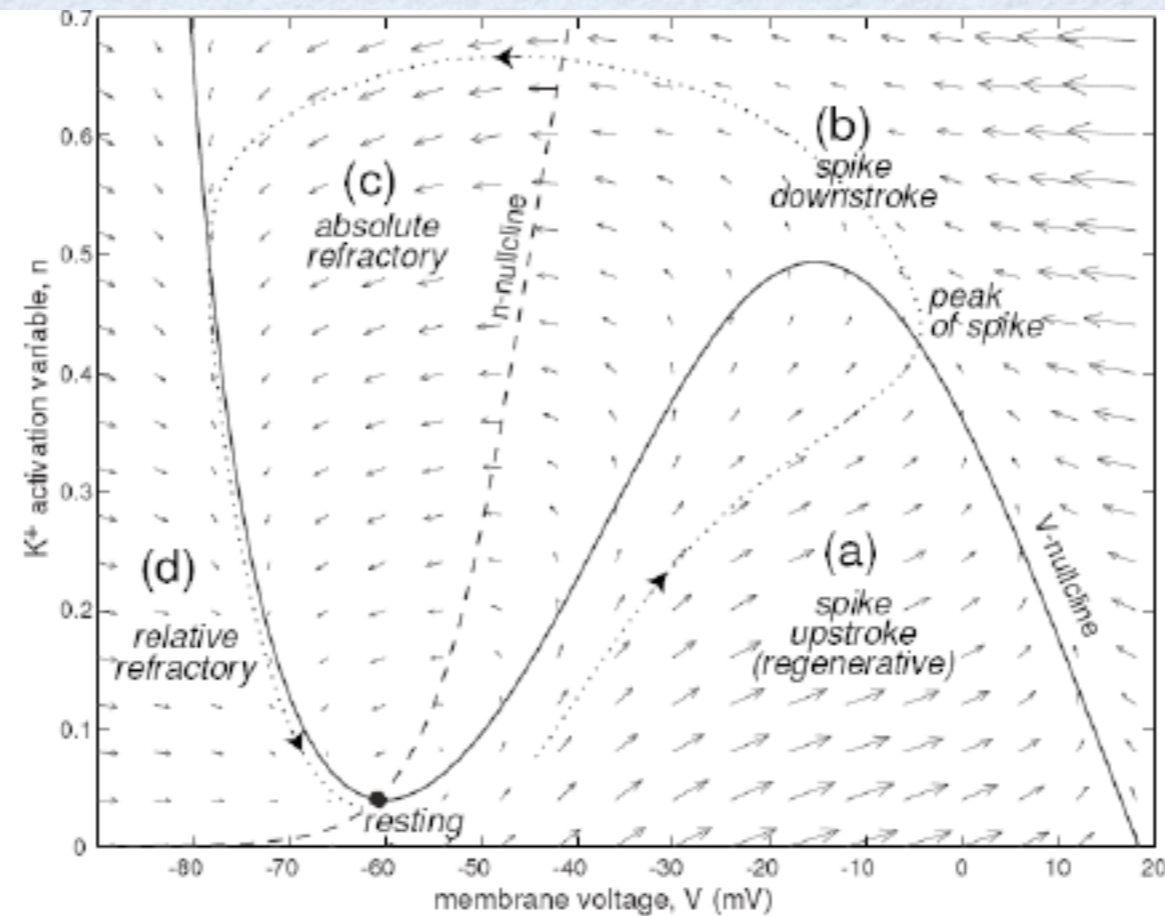
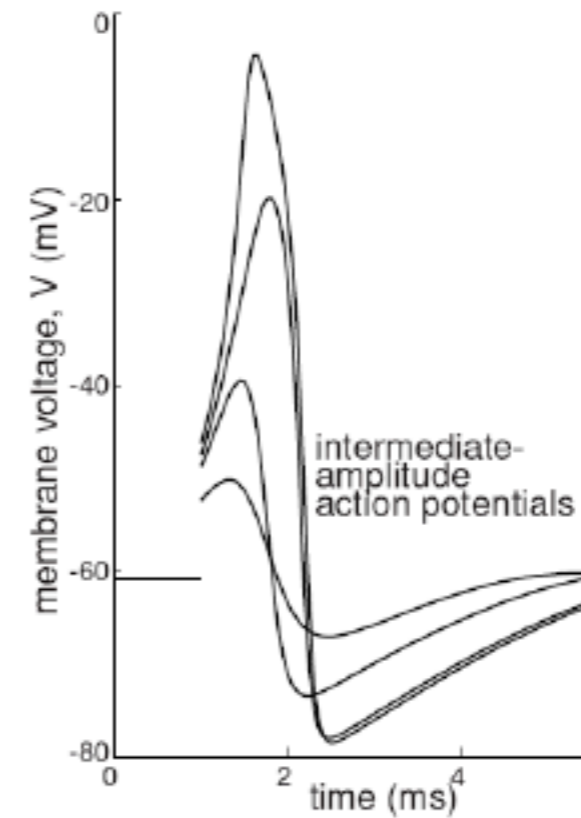
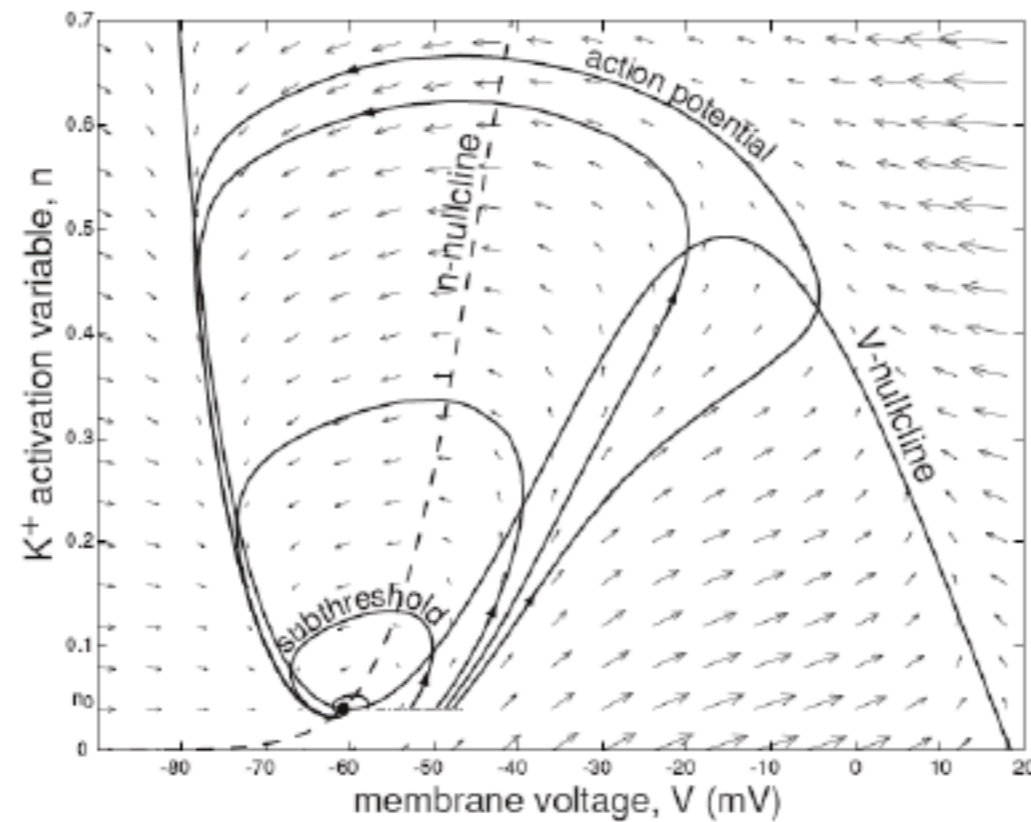


Figure 4.4: Nullclines of the  $I_{Na,p} + I_K$ -model (4.1, 4.2) with low-threshold  $K^+$  current in Fig. 4.1b. (The vector field is slightly distorted for the sake of clarity of illustration).

# Two-dimensional neural models

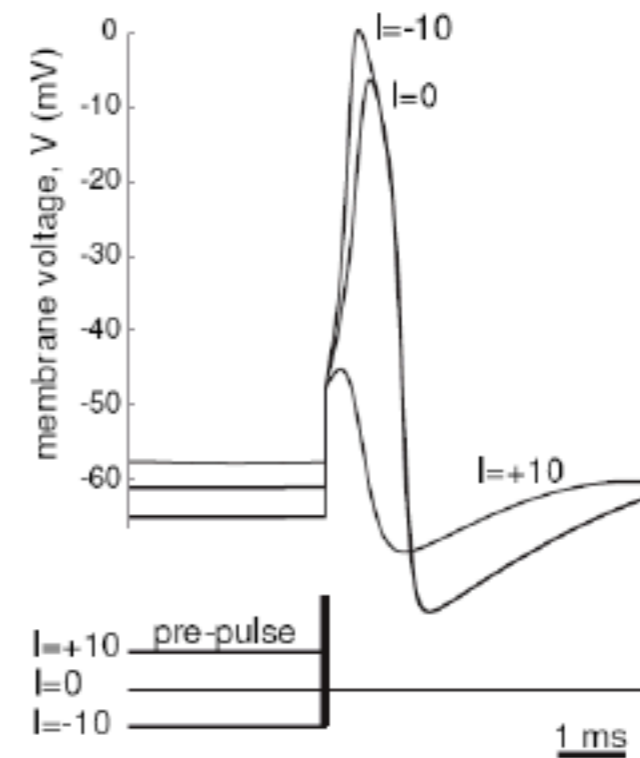
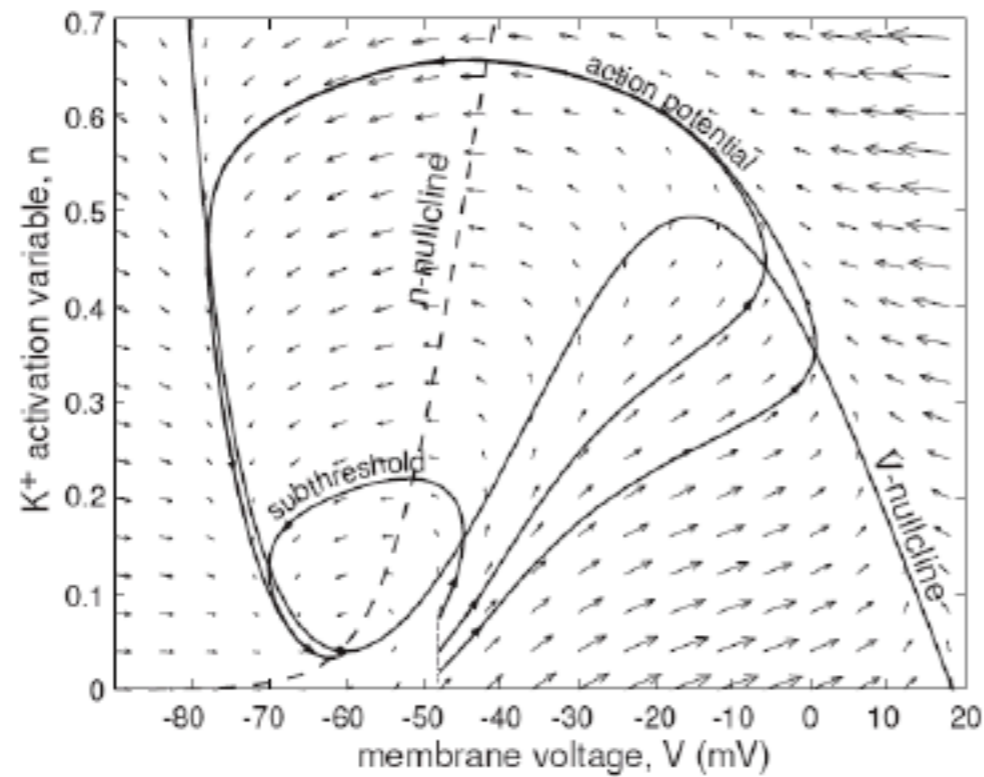
## Phase-plane



Failure to generate all-or-none action potentials in the  $I_{Na,p} + I_K$ -model

# Two-dimensional neural models

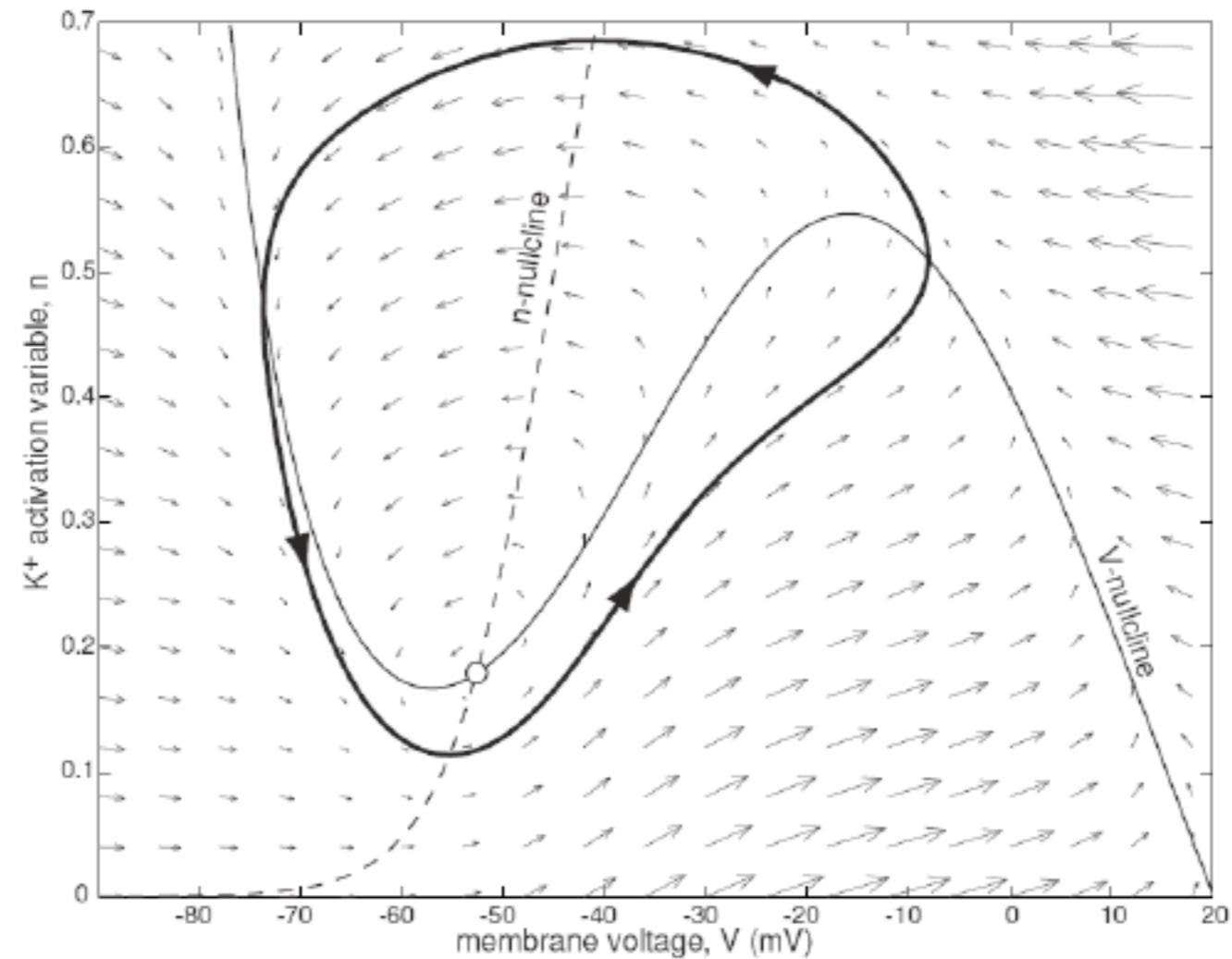
## Phase-plane



Failure to have a fixed value of threshold voltage in the  $I_{Na,p} + I_K$ -model

# Two-dimensional neural models

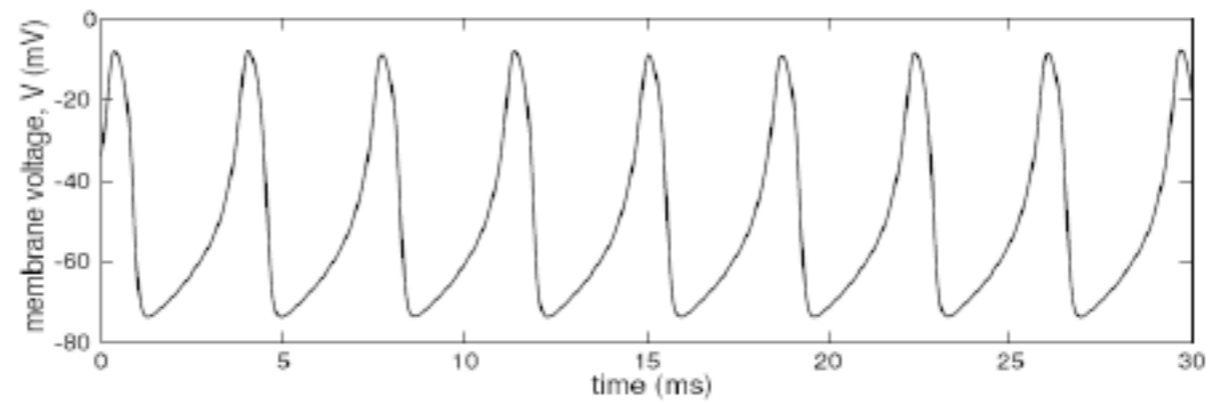
- Limit cycle in the  $I_{Na,p} + I_K$  model with low-threshold  $K^+$  and  $I = 40$





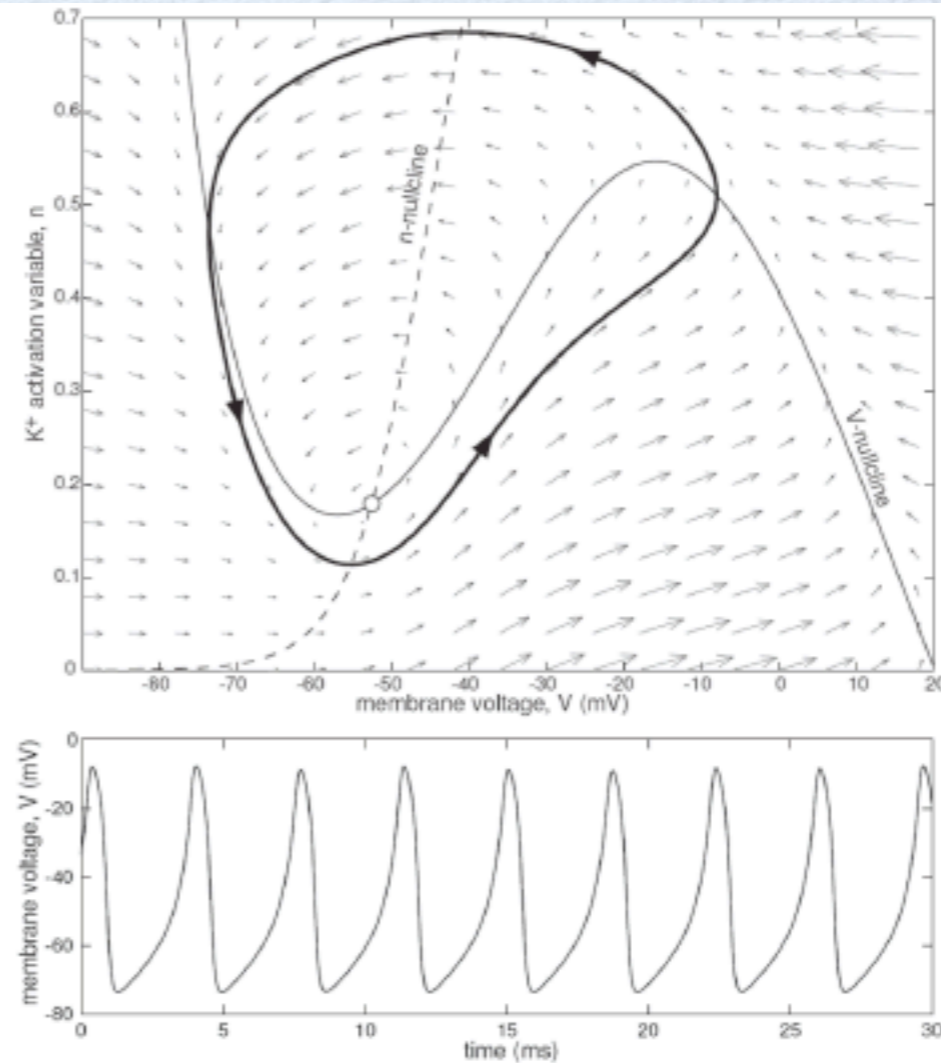
# Two-dimensional neural models

- Limit cycle in the  $I_{Na,p} + I_K$  model with low-threshold  $K^+$  and  $I = 40$



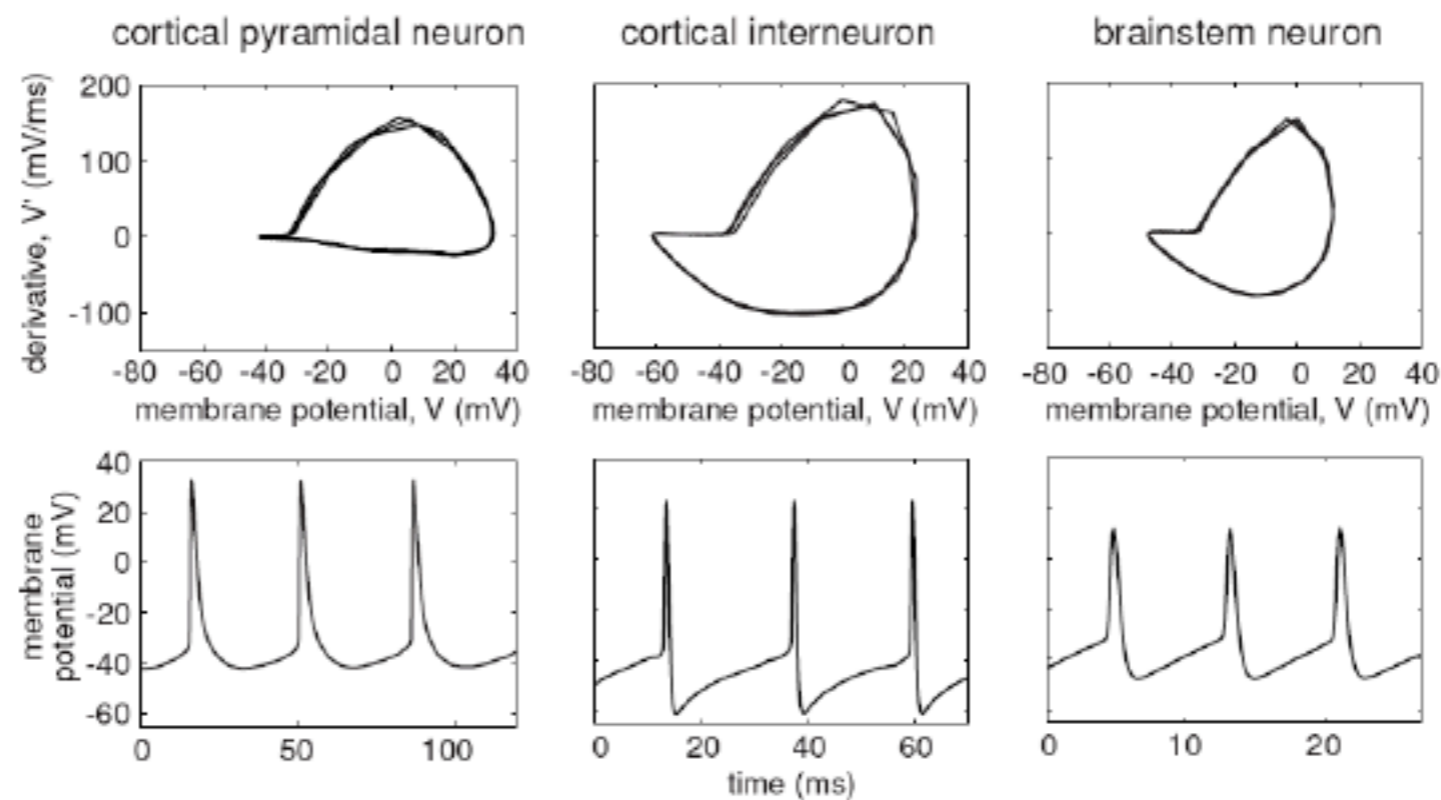
# Two-dimensional neural models

- Limit cycle in the  $I_{Na,p} + I_K$  model with low-threshold  $K^+$  and  $I = 40$



# Two-dimensional neural models

- Limit cycles corresponding to tonic spiking of three types of neurons recorded *in vitro*



# Two-dimensional neural models

## □ Relaxation oscillators

$$\frac{dx}{dt} = f(x, y)$$

$$\frac{dy}{dt} = \mu g(x, y)$$

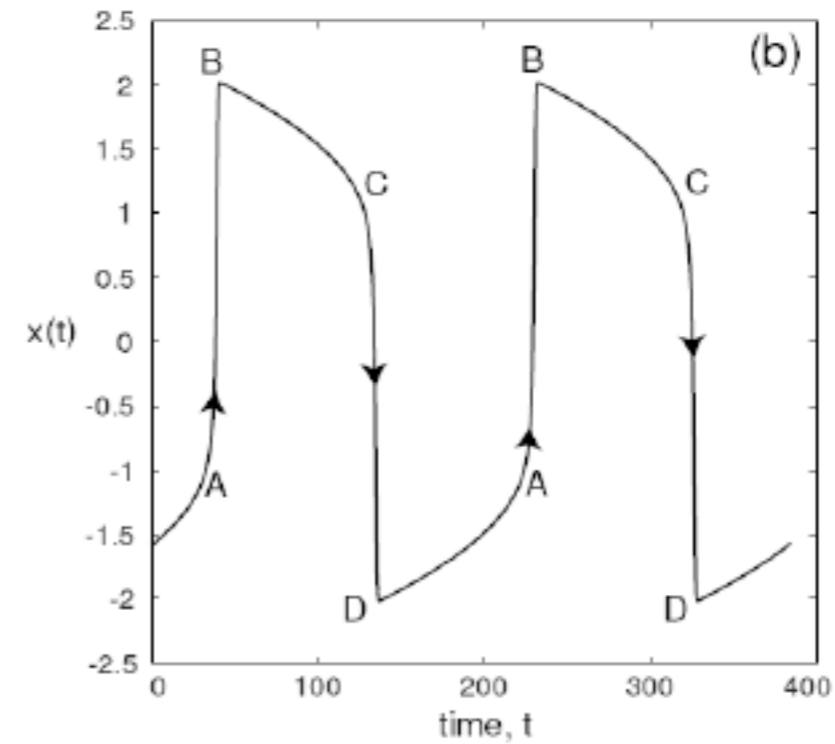
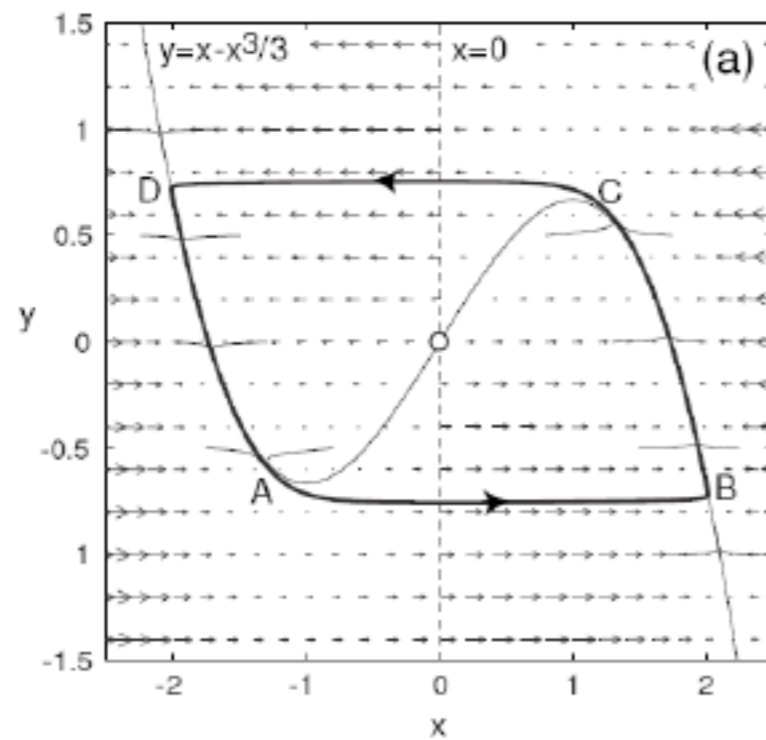
$$0 < \mu \ll 1$$

# Two-dimensional neural models

## □ Van de Pol model

$$\frac{dx}{dt} = x - x^3/3 - y$$

$$\frac{dy}{dt} = \mu x \quad \mu = 0.01$$



# Two-dimensional neural models

## □ Equilibria

$$\frac{dx}{dt} = f(x, y)$$

$$\frac{dy}{dt} = g(x, y)$$

$$f(x_0, y_0) = 0$$

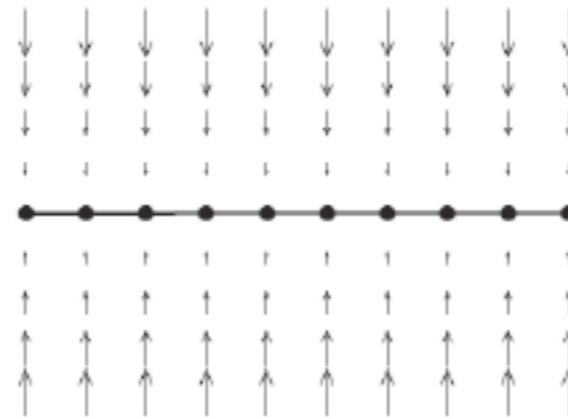
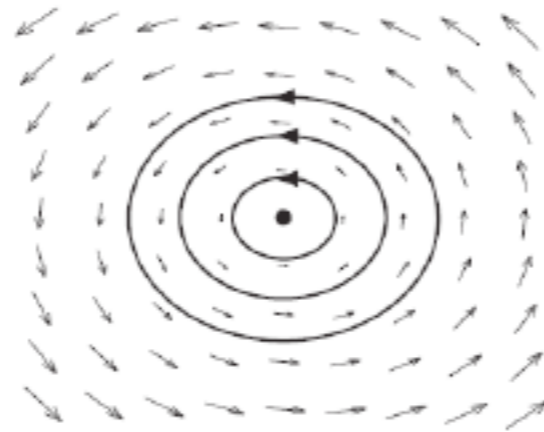
$$g(x_0, y_0) = 0$$

# Two-dimensional neural models

## □ Neutrally stable equilibria

$$\frac{dx}{dt} = f(x, y)$$

$$\frac{dy}{dt} = g(x, y)$$

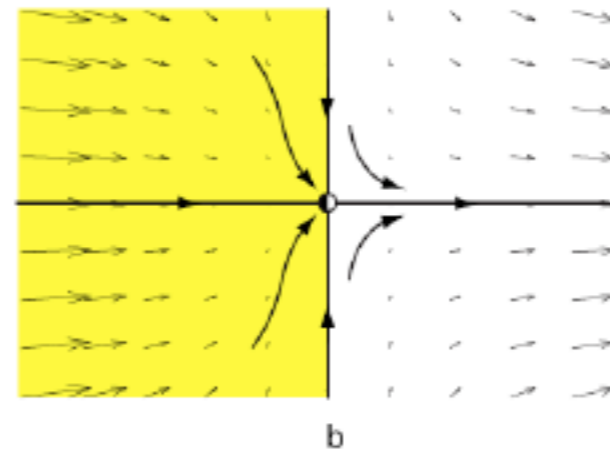
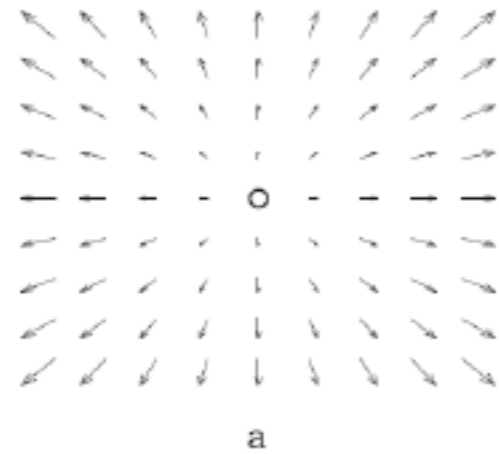


# Two-dimensional neural models

## □ Unstable equilibria

$$\frac{dx}{dt} = f(x, y)$$

$$\frac{dy}{dt} = g(x, y)$$





# Two-dimensional neural models

- Stable equilibria

$$\frac{dx}{dt} = f(x, y) \qquad \frac{dy}{dt} = g(x, y)$$

- Asymptotically stable
- Exponentially stable
- Neutrally stable

# Two-dimensional neural models

- Local linear analysis

$$\frac{dx}{dt} = f(x, y) \qquad \frac{dy}{dt} = g(x, y)$$

- Taylor expansion

$$f(x, y) = a(x - x_0) + b(y - y_0) + h.o.t.$$

$$g(x, y) = c(x - x_0) + d(y - y_0) + h.o.t.$$

$$a := f_x(x_0, y_0) \qquad b := f_y(x_0, y_0)$$

$$c := g_x(x_0, y_0) \qquad d := g_y(x_0, y_0)$$

# Two-dimensional neural models

## □ Local linear analysis

$$\mathbf{v} := \mathbf{x} - \mathbf{x}_0$$

$$\mathbf{w} := \mathbf{y} - \mathbf{y}_0$$

$$\begin{pmatrix} \mathbf{v}' \\ \mathbf{w}' \end{pmatrix} = \begin{pmatrix} a & b \\ c & d \end{pmatrix} \begin{pmatrix} \mathbf{v} \\ \mathbf{w} \end{pmatrix} = L \begin{pmatrix} \mathbf{v} \\ \mathbf{w} \end{pmatrix}$$

**$L$  : Jacobian Matrix**

$$\begin{pmatrix} \mathbf{v} \\ \mathbf{w} \end{pmatrix} = c_k \begin{pmatrix} u_v \\ u_w \end{pmatrix} e^{\lambda t} \quad k = 1, 2$$

# Two-dimensional neural models

## □ Eigenvalues and eigenvectors

$$L \begin{pmatrix} u_v \\ u_w \end{pmatrix} = \begin{pmatrix} a & b \\ c & d \end{pmatrix} \begin{pmatrix} u_v \\ u_w \end{pmatrix} = \lambda \begin{pmatrix} u_v \\ u_w \end{pmatrix}$$

$$(L - \lambda I) \begin{pmatrix} u_v \\ u_w \end{pmatrix} = \begin{pmatrix} 0 \\ 0 \end{pmatrix}$$

$$\det(L - \lambda I) = \begin{vmatrix} a - \lambda & b \\ c & d - \lambda \end{vmatrix} = 0$$

# Two-dimensional neural models

## □ Eigenvalues and eigenvectors

$$\lambda^2 - (a + d)\lambda + (ad - bc) = 0$$

$$\lambda^2 - \tau \lambda + \Delta = 0$$

$$\tau = a + d$$

$$\Delta = ad - bc$$

# Two-dimensional neural models

- Eigenvalues and eigenvectors

$$\lambda_1 = \frac{\tau + \sqrt{\tau^2 - 4\Delta}}{2}$$

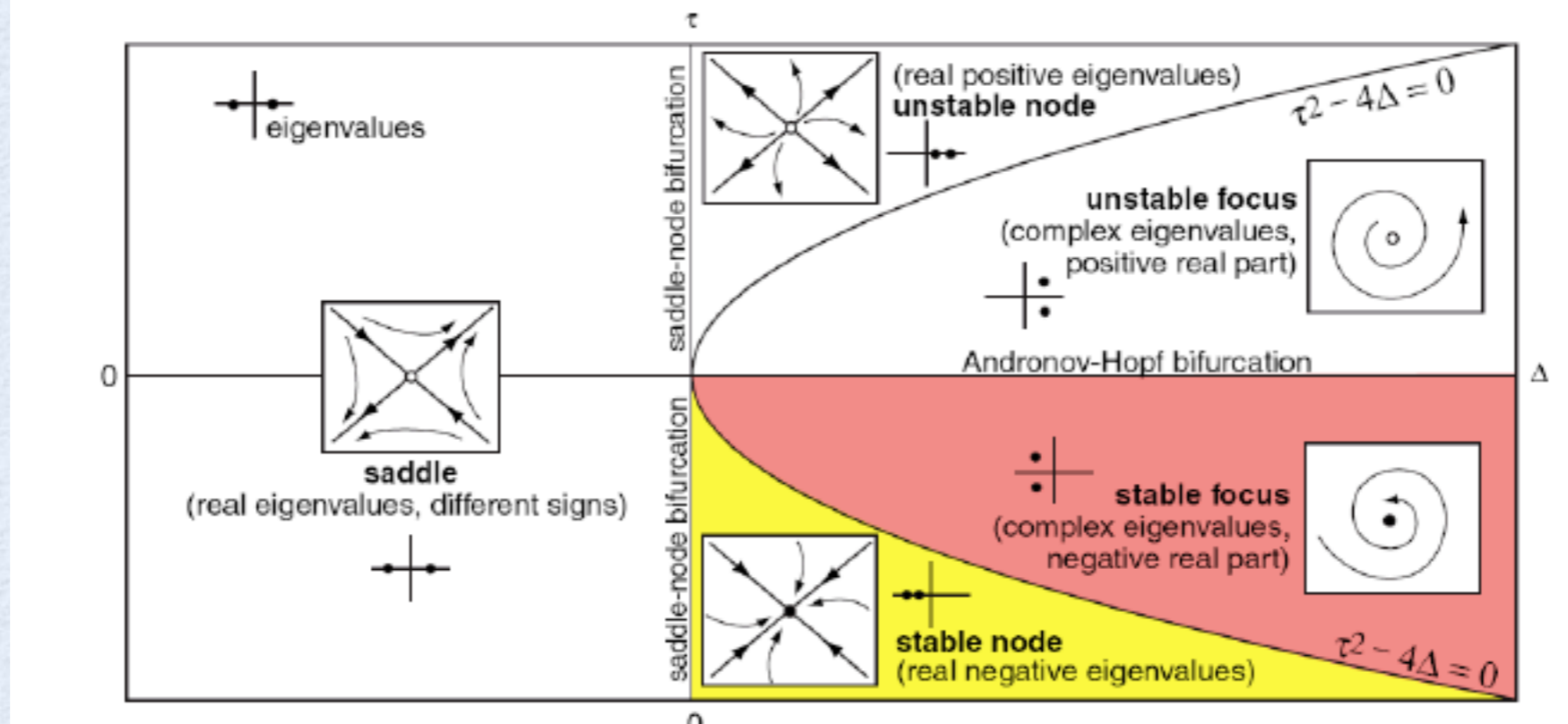
$$\lambda_2 = \frac{\tau - \sqrt{\tau^2 - 4\Delta}}{2}$$

$$\begin{pmatrix} v \\ w \end{pmatrix} = c_1 \begin{pmatrix} u_{v,1} \\ u_{w,1} \end{pmatrix} e^{\lambda_1 t} + c_2 \begin{pmatrix} u_{v,2} \\ u_{w,2} \end{pmatrix} e^{\lambda_2 t}$$

# Two-dimensional neural models

$$\lambda_{1,2} = \frac{\tau \pm \sqrt{\tau^2 - 4\Delta}}{2}$$

$$\begin{pmatrix} v \\ w \end{pmatrix} = c_1 \begin{pmatrix} u_{v,1} \\ u_{w,1} \end{pmatrix} e^{\lambda_1 t} + c_2 \begin{pmatrix} u_{v,2} \\ u_{w,2} \end{pmatrix} e^{\lambda_2 t}$$



# Two-dimensional neural models

$$\square \lambda_{1,2} = \frac{\tau \pm \sqrt{\tau^2 - 4\Delta}}{2} \quad \begin{pmatrix} v \\ w \end{pmatrix} = c_1 \begin{pmatrix} u_{v,1} \\ u_{w,1} \end{pmatrix} e^{\lambda_1 t} + c_2 \begin{pmatrix} u_{v,2} \\ u_{w,2} \end{pmatrix} e^{\lambda_2 t}$$

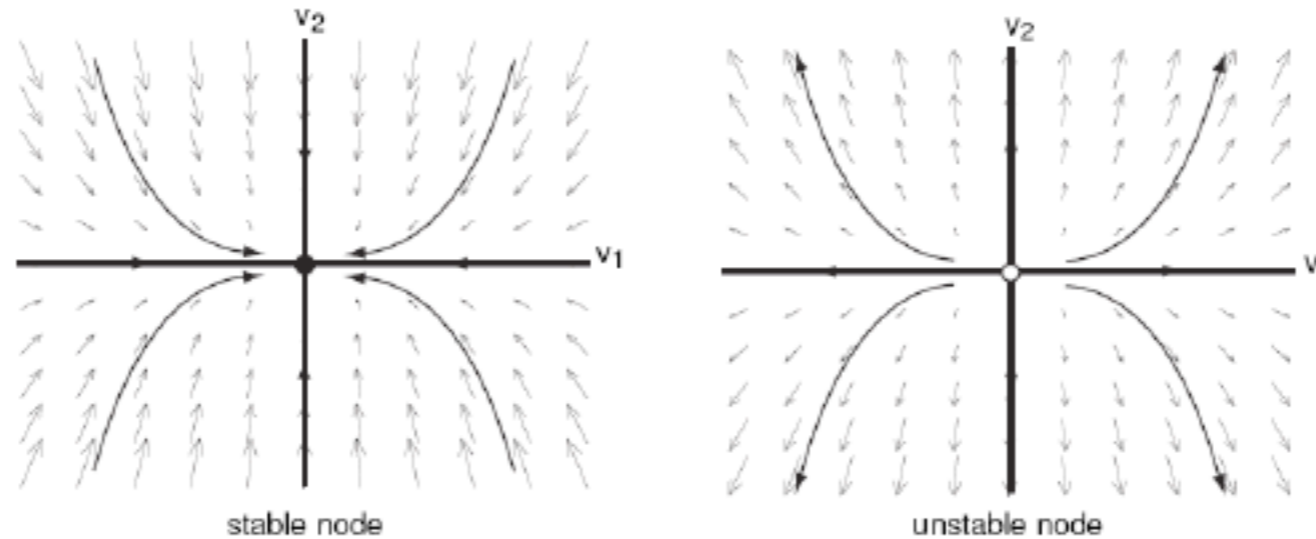


Figure 4.16: Node equilibrium occurs when both eigenvalues are real and have the same sign, e.g.,  $\lambda_1 = -1$  and  $\lambda_2 = -3$  (stable) or  $\lambda_1 = +1$  and  $\lambda_2 = +3$  (unstable). Most trajectories converge to or diverge from the node along the eigenvector  $v_1$  corresponding to the eigenvalue having the smallest absolute value.



# Two-dimensional neural models

$$\square \lambda_{1,2} = \frac{\tau \pm \sqrt{\tau^2 - 4\Delta}}{2} \quad \begin{pmatrix} v \\ w \end{pmatrix} = c_1 \begin{pmatrix} u_{v,1} \\ u_{w,1} \end{pmatrix} e^{\lambda_1 t} + c_2 \begin{pmatrix} u_{v,2} \\ u_{w,2} \end{pmatrix} e^{\lambda_2 t}$$

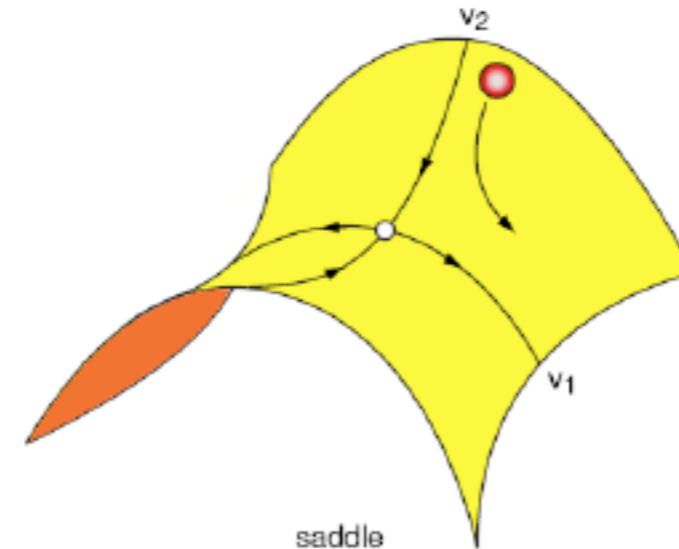
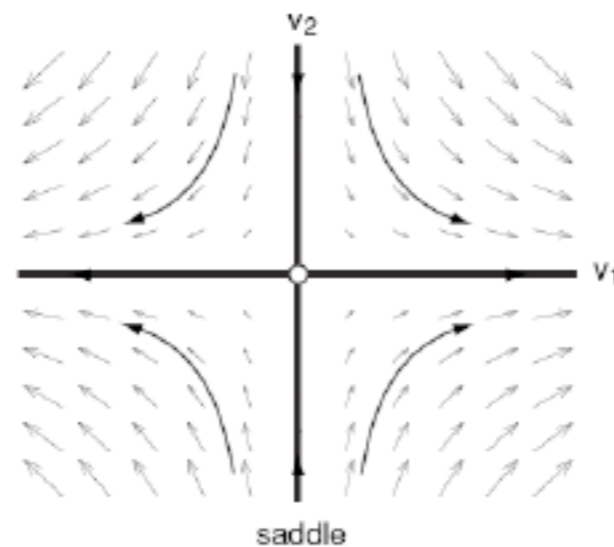
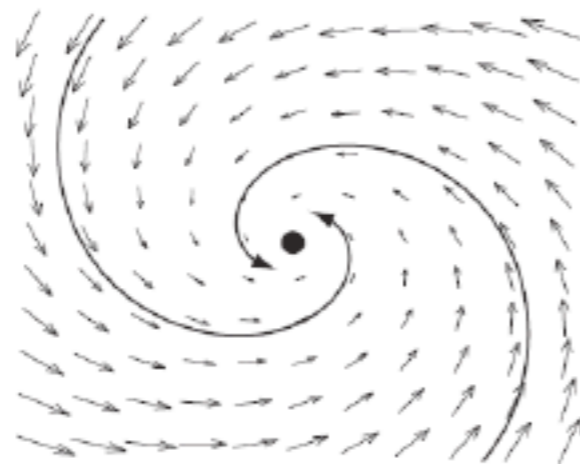


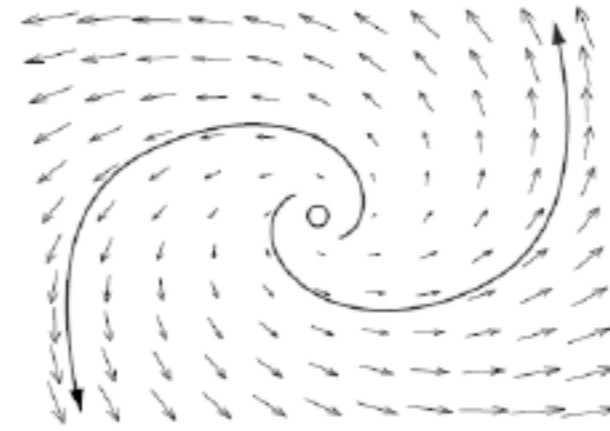
Figure 4.17: Saddle equilibrium occurs when two real eigenvalues have opposite signs, e.g.,  $\lambda_1 = +1$  and  $\lambda_2 = -1$ . Most trajectories diverge from the equilibrium along the eigenvector corresponding to the positive eigenvalue (in this case  $v_1$ ).

# Two-dimensional neural models

$$\square \lambda_{1,2} = \frac{\tau \pm \sqrt{\tau^2 - 4\Delta}}{2} \quad \begin{pmatrix} v \\ w \end{pmatrix} = c_1 \begin{pmatrix} u_{v,1} \\ u_{w,1} \end{pmatrix} e^{\lambda_1 t} + c_2 \begin{pmatrix} u_{v,2} \\ u_{w,2} \end{pmatrix} e^{\lambda_2 t}$$



stable focus

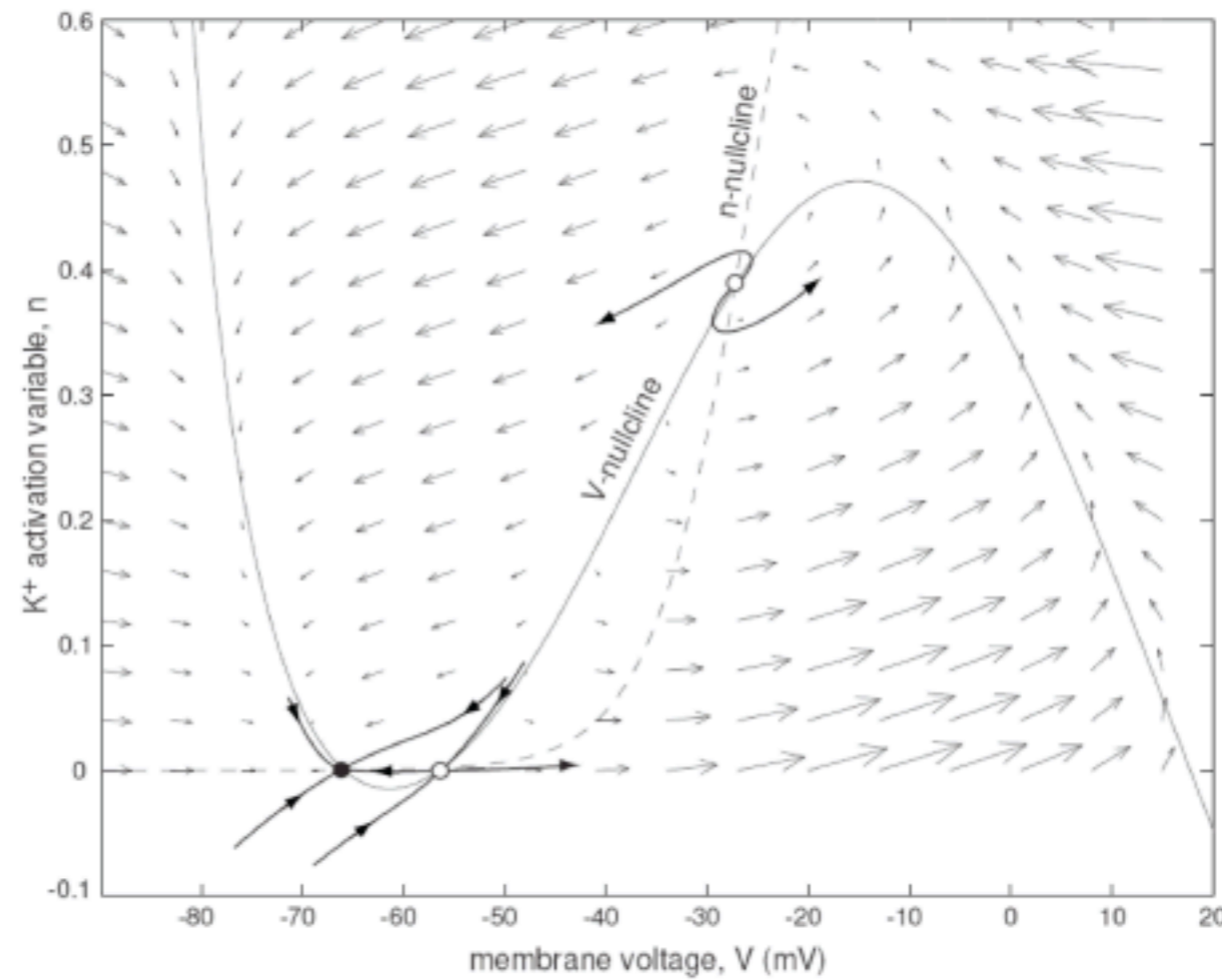


unstable focus

Figure 4.18: Focus equilibrium occurs when the eigenvalues are complex-conjugate, e.g.,  $\lambda = -3 \pm i$  (stable) or  $\lambda = +3 \pm i$  (unstable). The imaginary part (here 1) determines the frequency of rotation around the focus.

# Two-dimensional neural models

- Phase portrait of the  $I_{Na,p} + I_K$  model with high-threshold  $K^+$  current



# Two-dimensional neural models

- FitzHugh-Nagumo model

$$V' = V(a - V)(V - 1) - w + I$$

$$w' = bV - cw$$

- Nullclines

$$w = V(a - V)(V - 1) + I$$

$$w = \frac{b}{c}V$$

$$\tau = -a - c$$

$$\Delta = ac + b$$

# Two-dimensional neural models

## □ FitzHugh-Nagumo model

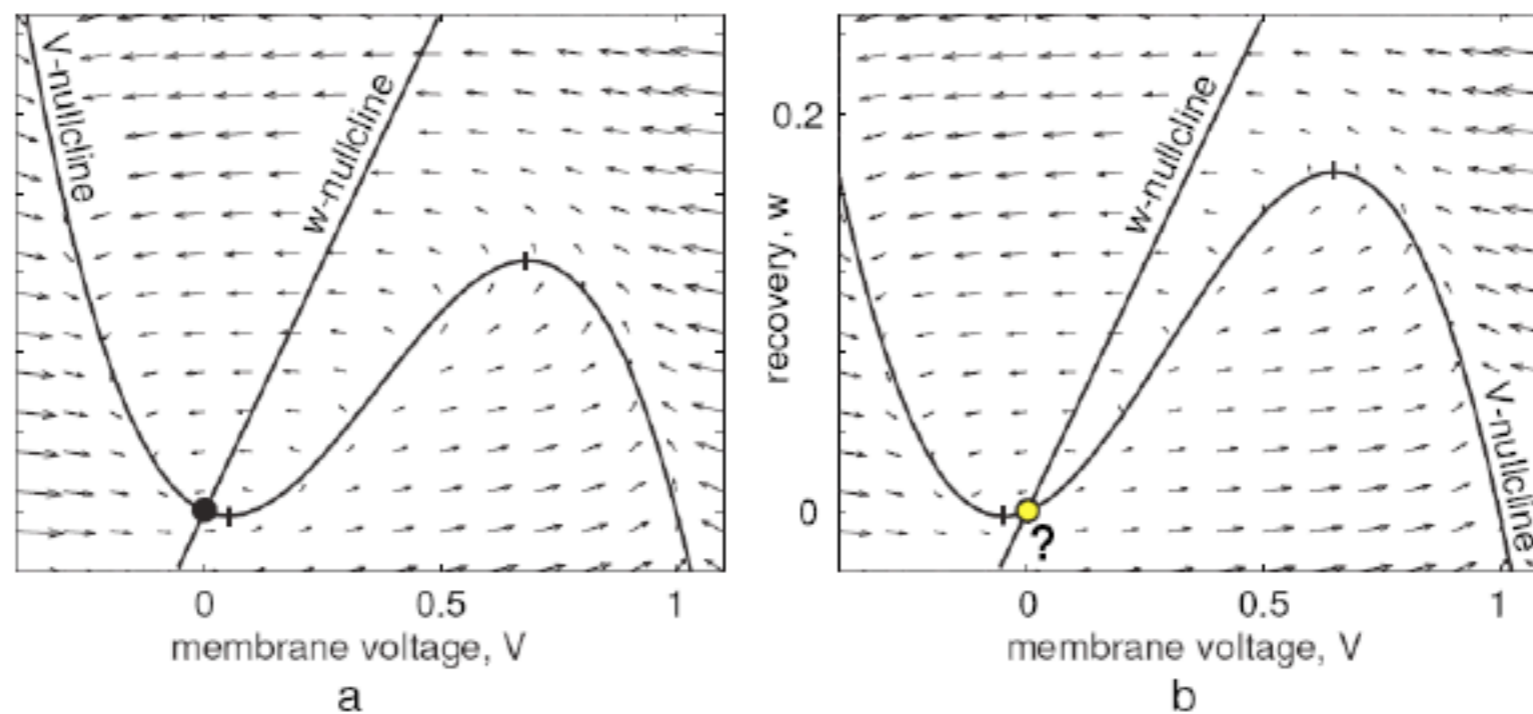


Figure 4.20: Nullclines in the FitzHugh-Nagumo model (4.11, 4.12). Parameters:  $I = 0, b = 0.01, c = 0.02, a = 0.1$  (left) and  $a = -0.1$  (right).

# Two-dimensional neural models

## □ FitzHugh-Nagumo model

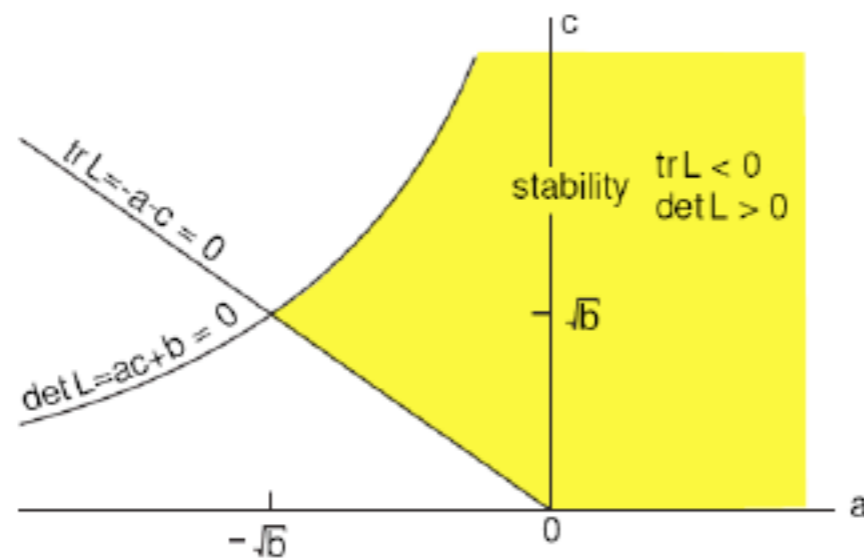


Figure 4.21: Stability diagram of the equilibrium  $(0,0)$  in the FitzHugh-Nagumo model (4.11,4.12).

# Two-dimensional neural models

## □ FitzHugh-Nagumo model

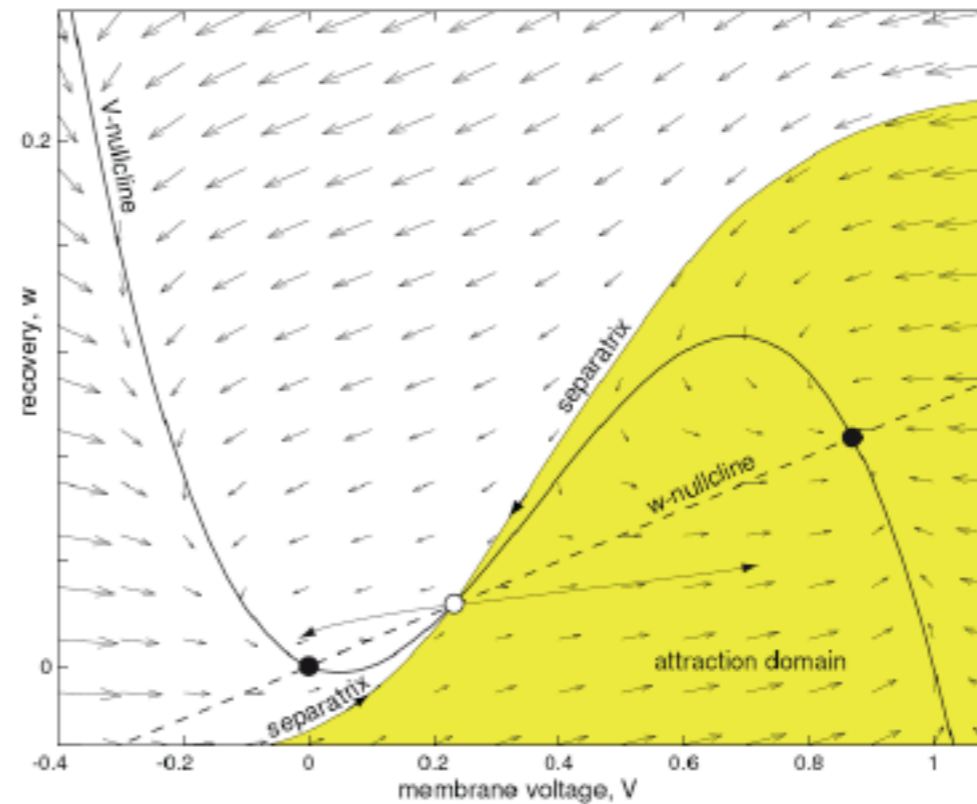


Figure 4.22: Bistability of two equilibrium attractors (black circles) in the FitzHugh-Nagumo model (4.11,4.12). The shaded area — attraction domain of the right equilibrium. Parameters:  $I = 0$ ,  $b = 0.01$ ,  $a = c = 0.1$ .

# Two-dimensional neural models

## □ Bistability

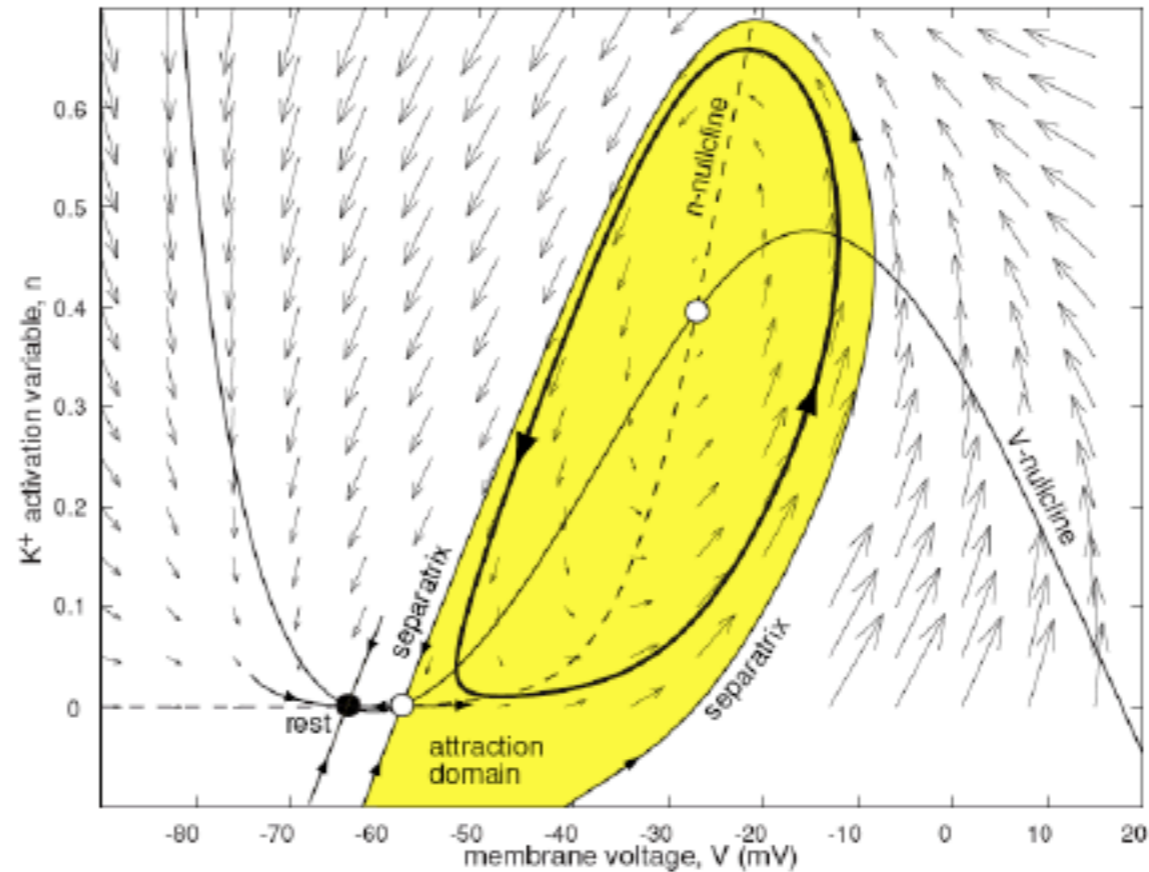


Figure 4.23: Bistability of rest and spiking states in the  $I_{Na,P} + I_K$ -model (4.1, 4.2) with high-threshold fast ( $\tau(V) = 0.152$ )  $K^+$  current and  $I = 3$ . A brief strong pulse of current (arrow) brings the state vector of the system into the attraction domain of the stable limit cycle.



# Two-dimensional neural models

## □ Bistability

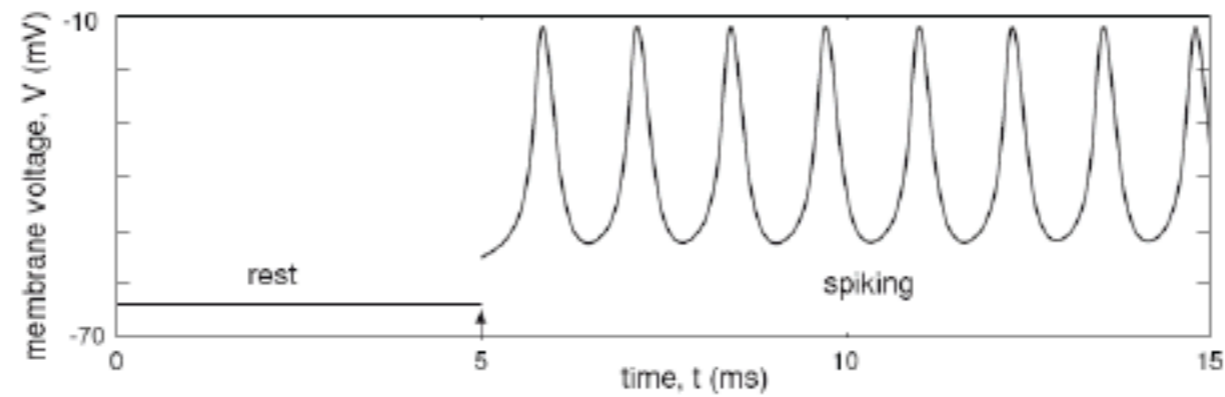


Figure 4.23: Bistability of rest and spiking states in the  $I_{Na,p} + I_K$ -model (4.1, 4.2) with high-threshold fast ( $\tau(V) = 0.152$ )  $K^+$  current and  $I = 3$ . A brief strong pulse of current (arrow) brings the state vector of the system into the attraction domain of the stable limit cycle.

# Two-dimensional neural models

## □ Stable and unstable manifolds

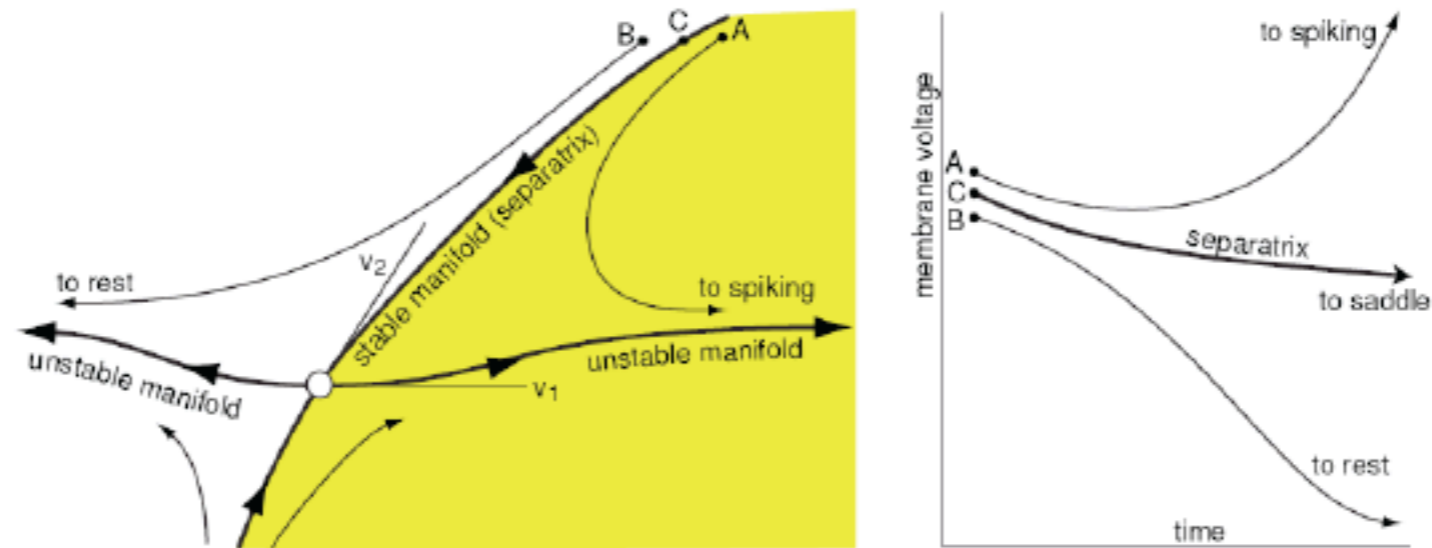


Figure 4.24: Stable and unstable manifolds to a saddle. The eigenvectors  $v_1$  and  $v_2$  correspond to positive and negative eigenvalues, respectively.

# Two-dimensional neural models

## □ Homoclinic and heteroclinic trajectories

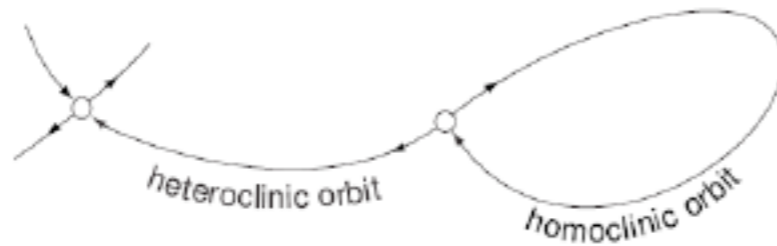


Figure 4.25: A heteroclinic orbit starts and ends at different equilibria. A homoclinic orbit starts and ends at the same equilibrium.

# Two-dimensional neural models

- Homoclinic and heteroclinic trajectories

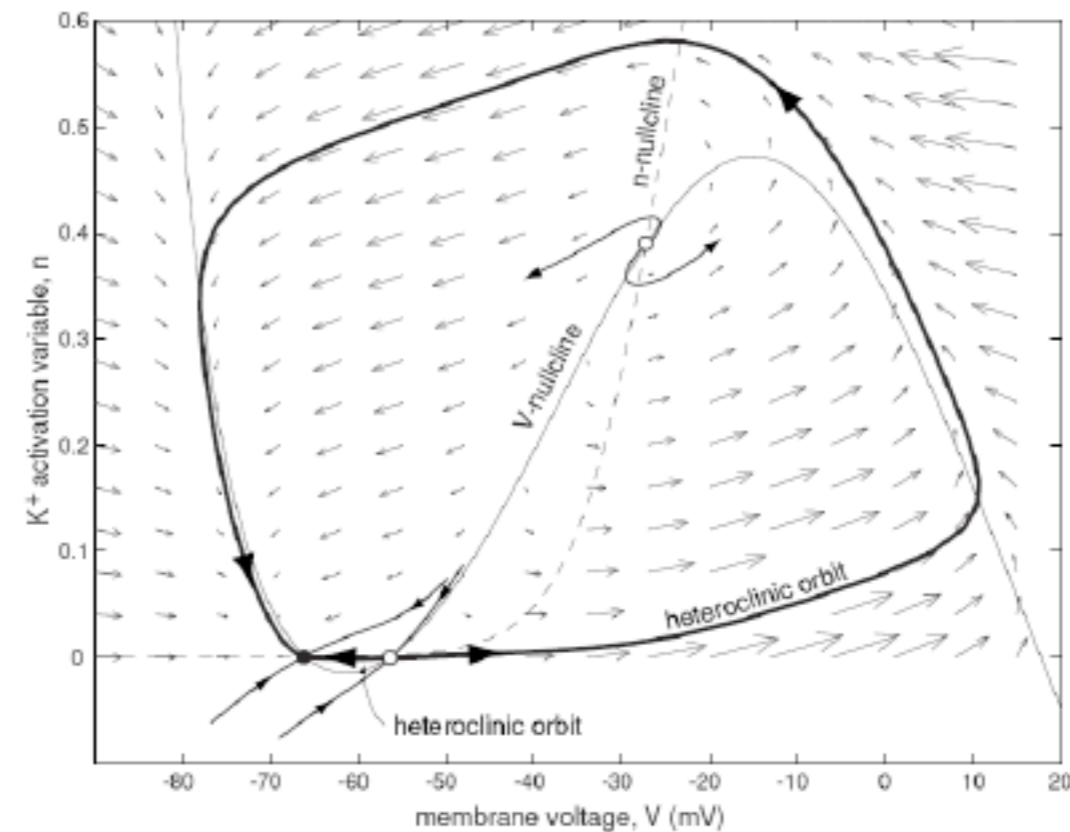


Figure 4.26: Two heteroclinic orbits (bold curves connecting stable and unstable equilibria) in the  $I_{Na,p} + I_K$ -model with high-threshold  $K^+$  current.

# Two-dimensional neural models

## □ Homoclinic and heteroclinic trajectories

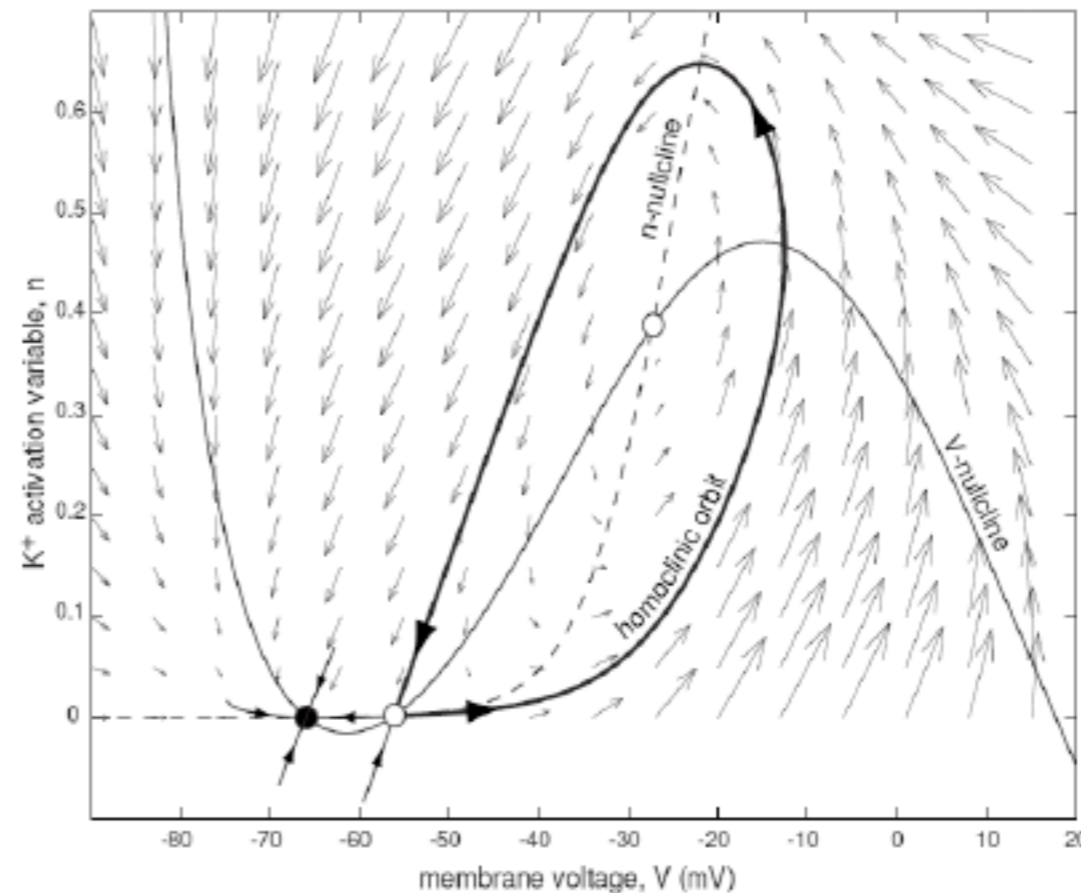


Figure 4.27: Homoclinic orbit (bold) in the  $I_{Na,p}+I_K$ -model with high-threshold fast ( $\tau(V) = 0.152$ )  $K^+$  current.

# Two-dimensional neural models

- Homoclinic and heteroclinic trajectories

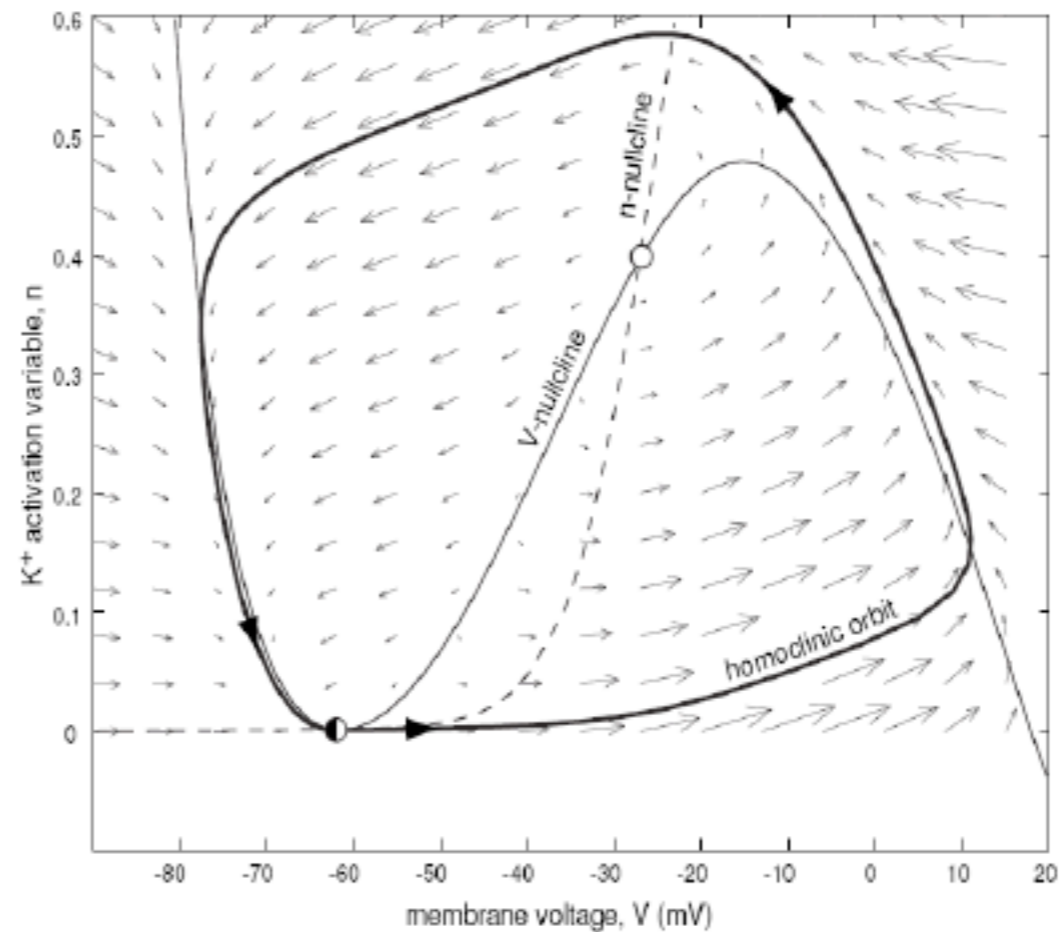
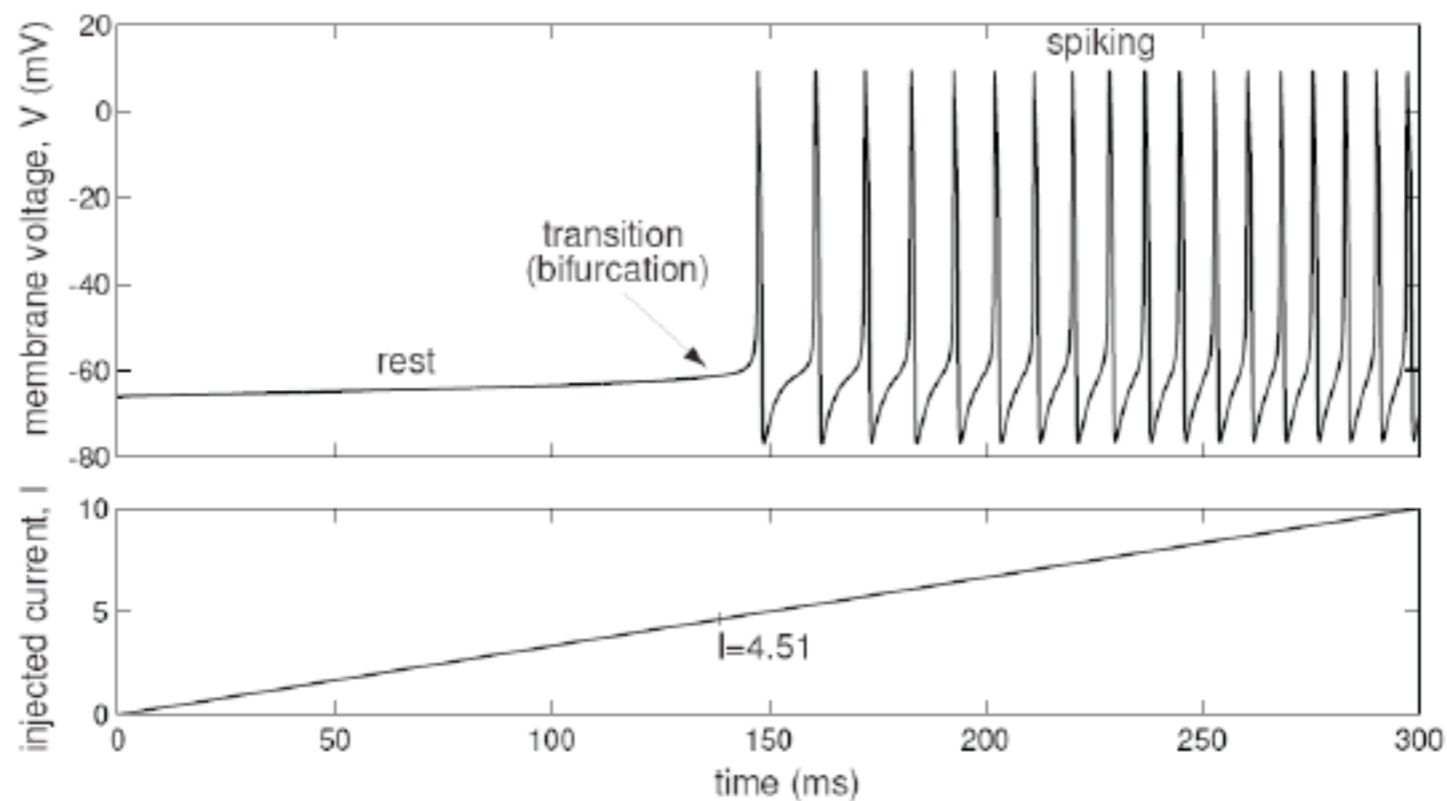


Figure 4.28: Homoclinic orbit (bold) to saddle-node equilibrium in the  $I_{Na,p} + I_K$ -model with high-threshold  $K^+$  current and  $I = 4.51$ .

# Two-dimensional neural models

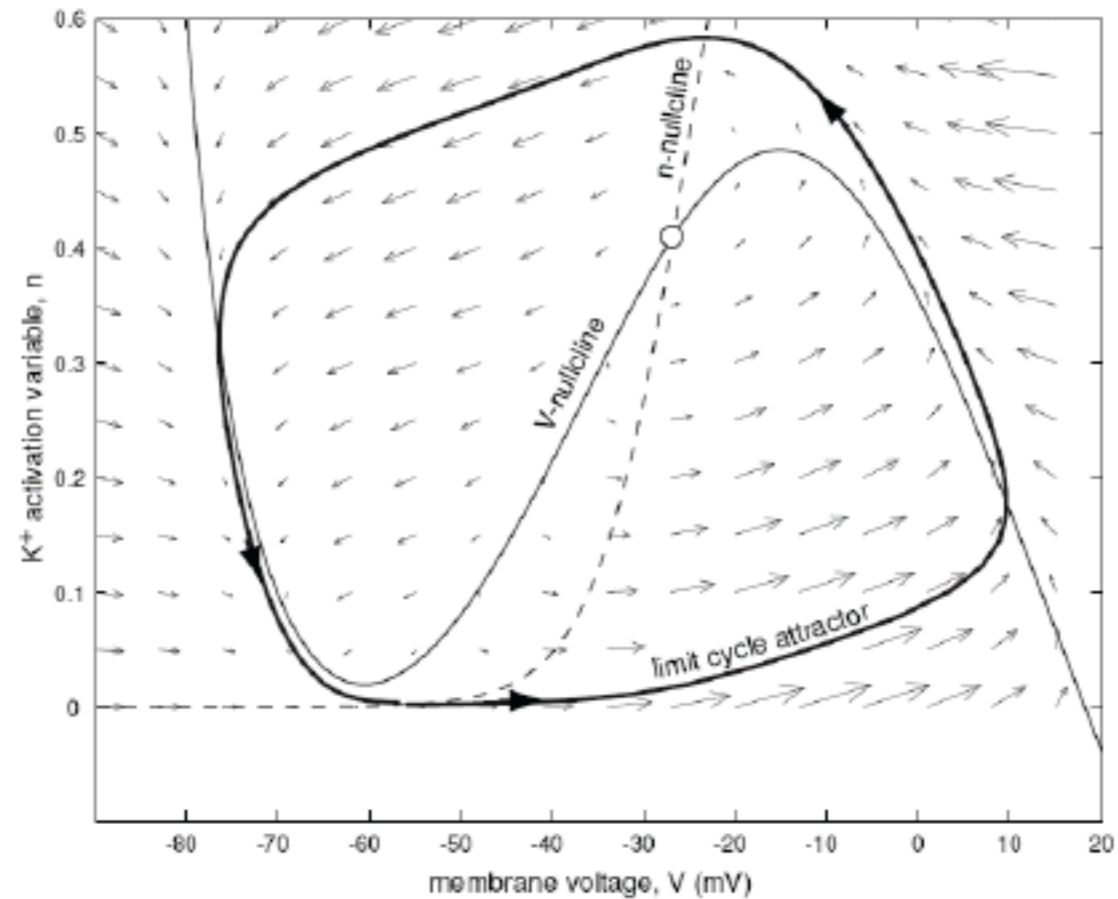
## □ Saddle-node bifurcation



Transition from rest state to repetitive spiking in the  $I_{Na,p} + I_K$ -model

# Two-dimensional neural models

## □ Limit cycle attractor

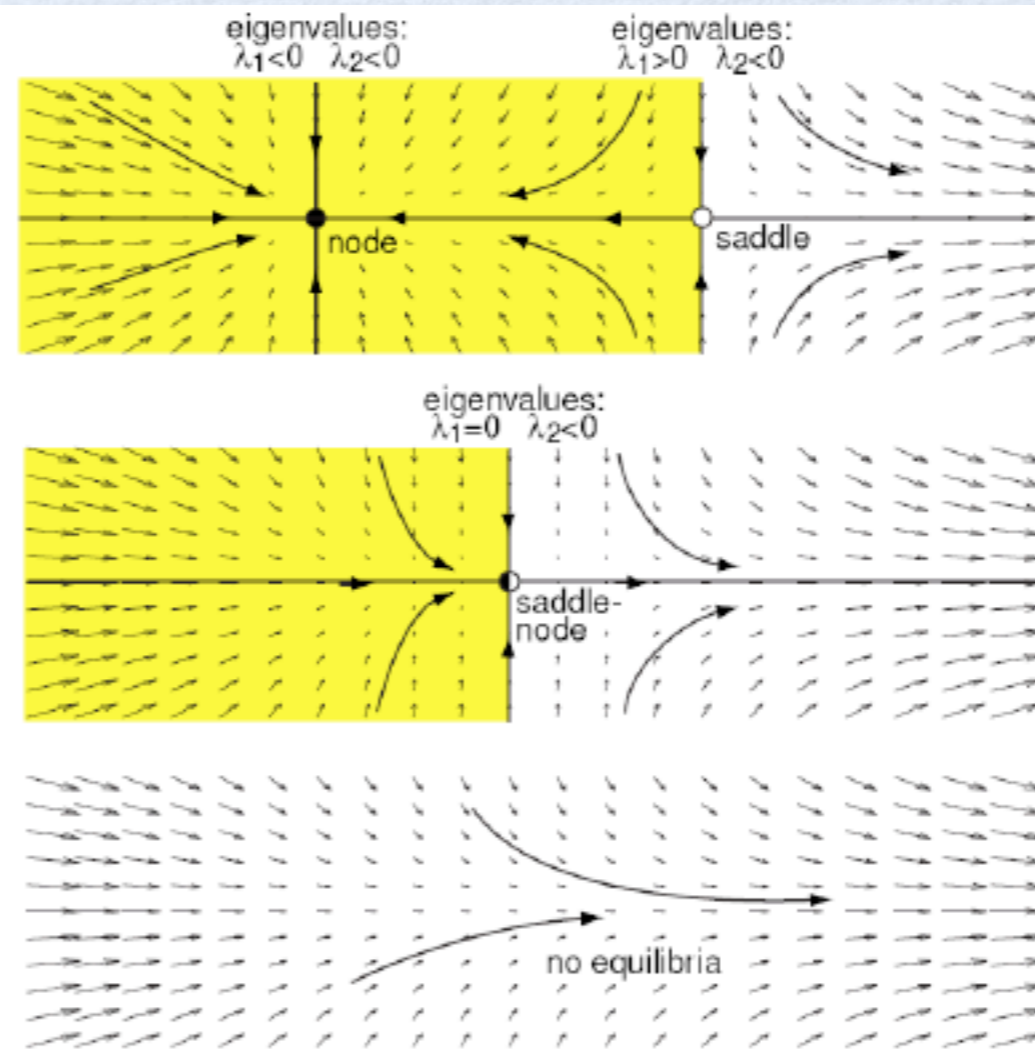


Limit cycle attractor (bold) in the  $I_{Na,p} + I_K$ -model when  $I = 10$



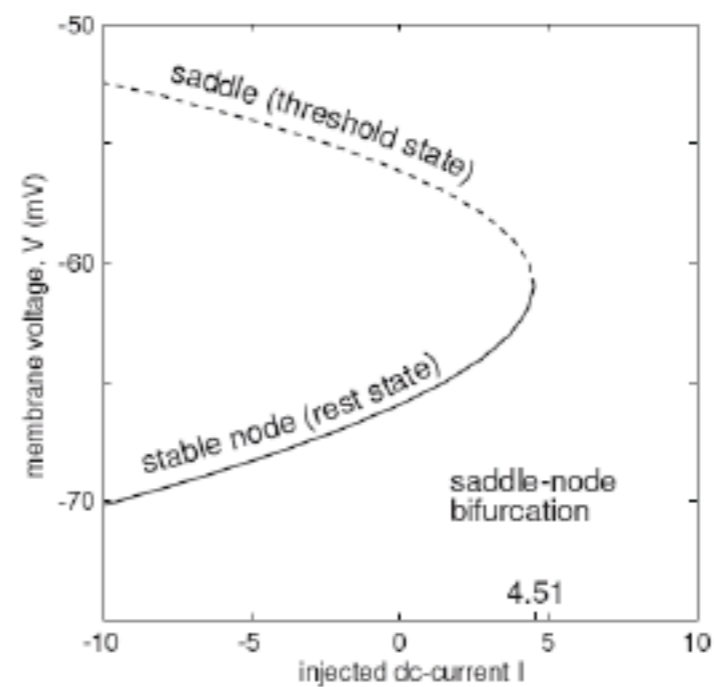
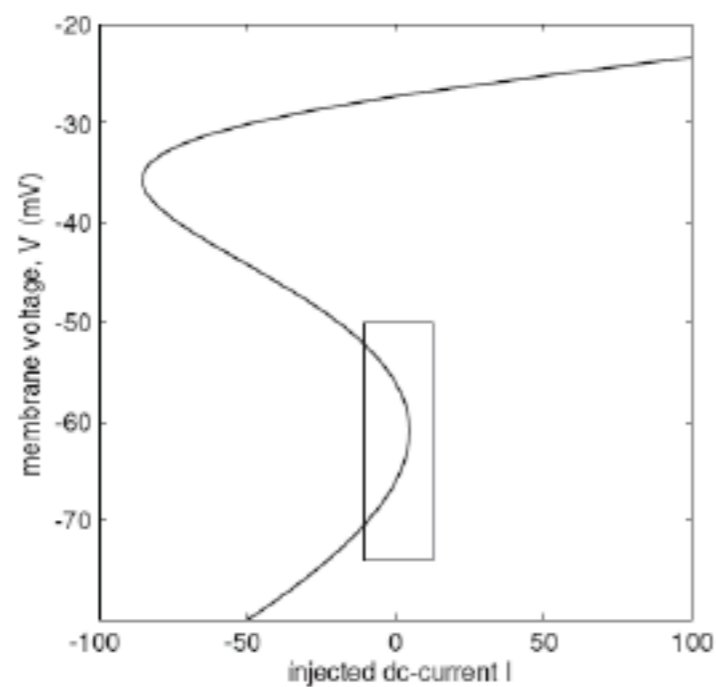
# Two-dimensional neural models

## □ Saddle-node bifurcation



# Two-dimensional neural models

## □ Saddle-node bifurcation in the $I_{na,p} + I_K$ model



# Two-dimensional neural models

## □ Saddle-node bifurcation in the $I_{Na,p} + I_K$ model

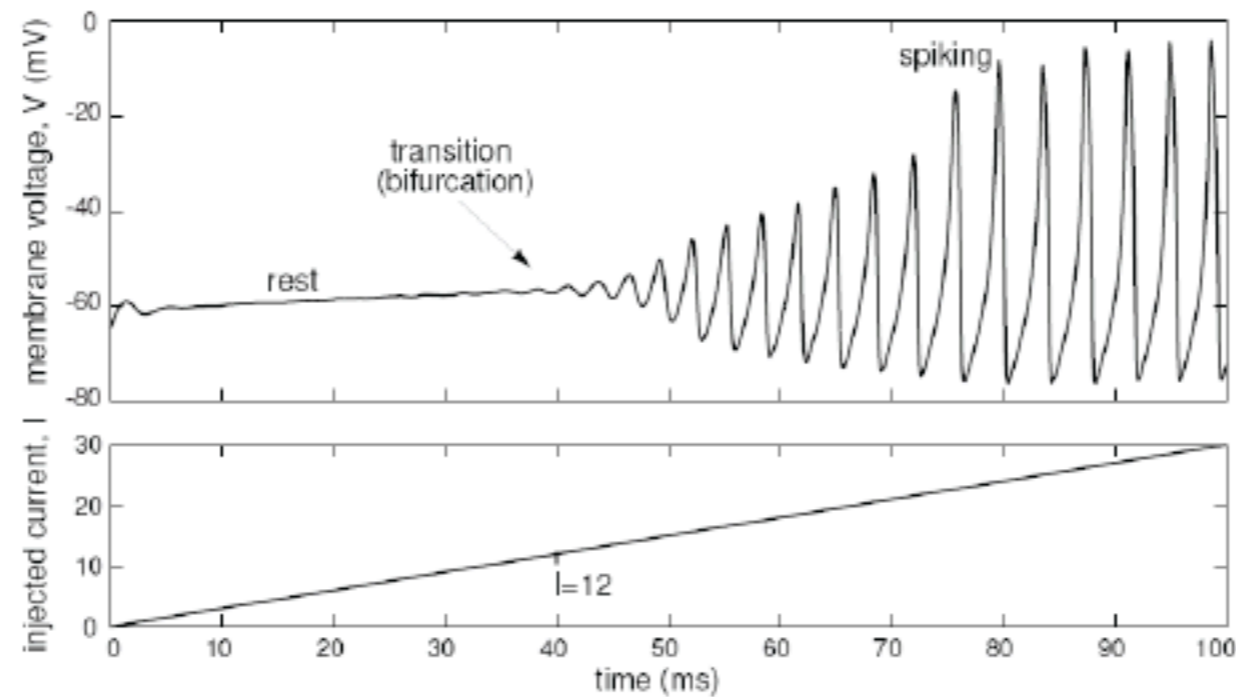
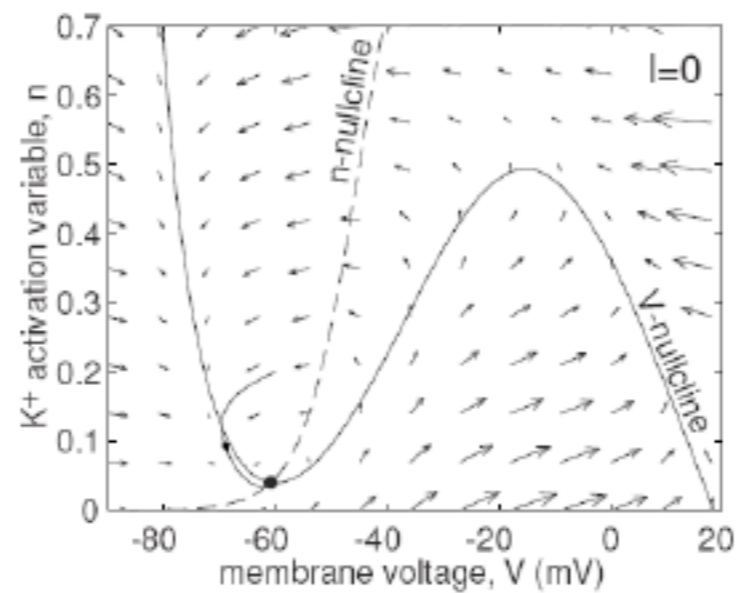


Figure 4.33: Transition from rest state to repetitive spiking in the  $I_{Na,p} + I_K$ -model with ramp injected current  $I$ ; see also Fig. 4.34 (small-amplitude noise is added to the model to mask the slow passage effect). Notice that the frequency of spiking is relatively constant for a wide range of injected current.

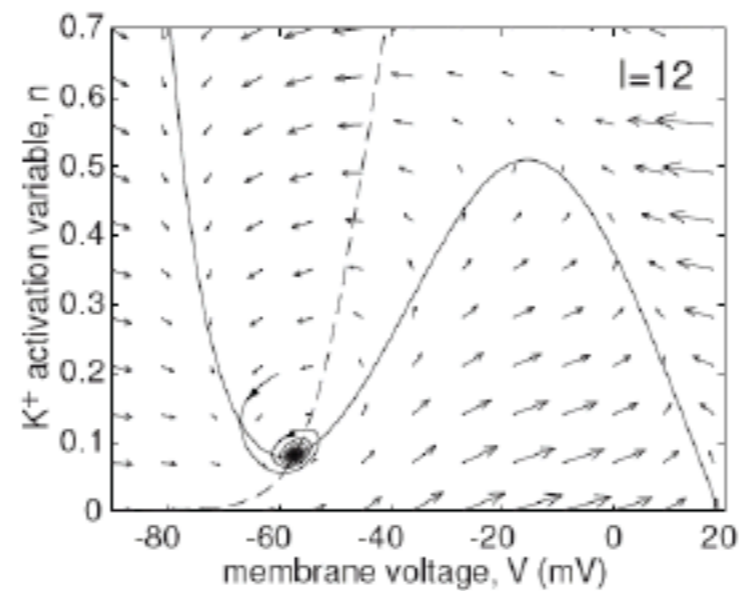
# Two-dimensional neural models

- Supercritical Hopf bifurcation in the  $I_{na,p} + I_K$  model with low-threshold  $K^+$  current when  $I=12$



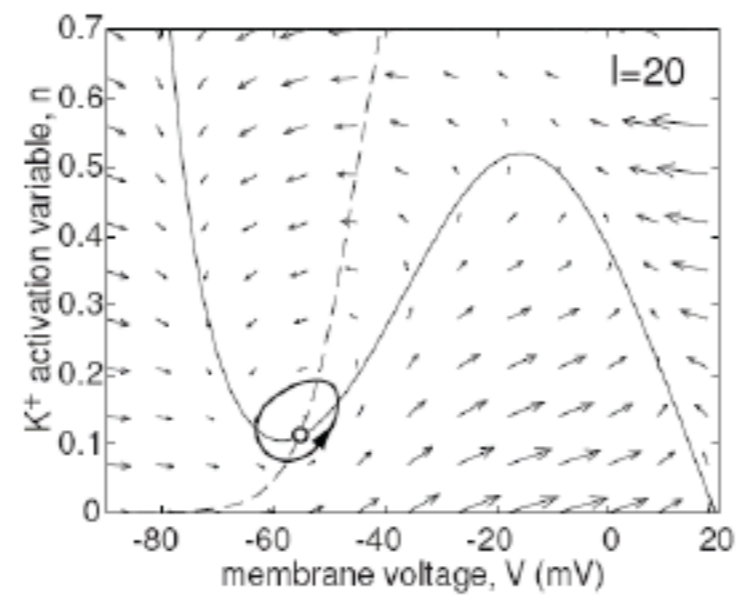
# Two-dimensional neural models

- Supercritical Hopf bifurcation in the  $I_{na,p} + I_K$  model with low-threshold  $K^+$  current when  $I=12$



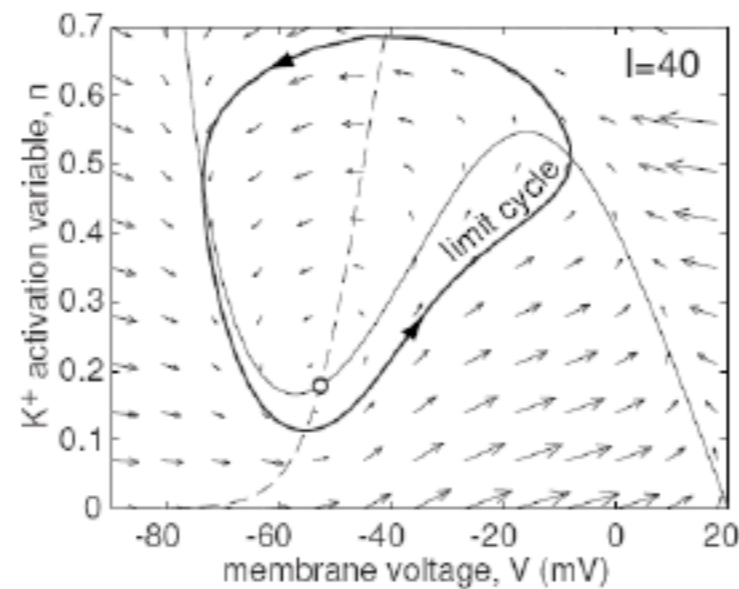
# Two-dimensional neural models

- Supercritical Hopf bifurcation in the  $I_{na,p} + I_K$  model with low-threshold  $K^+$  current when  $I=12$



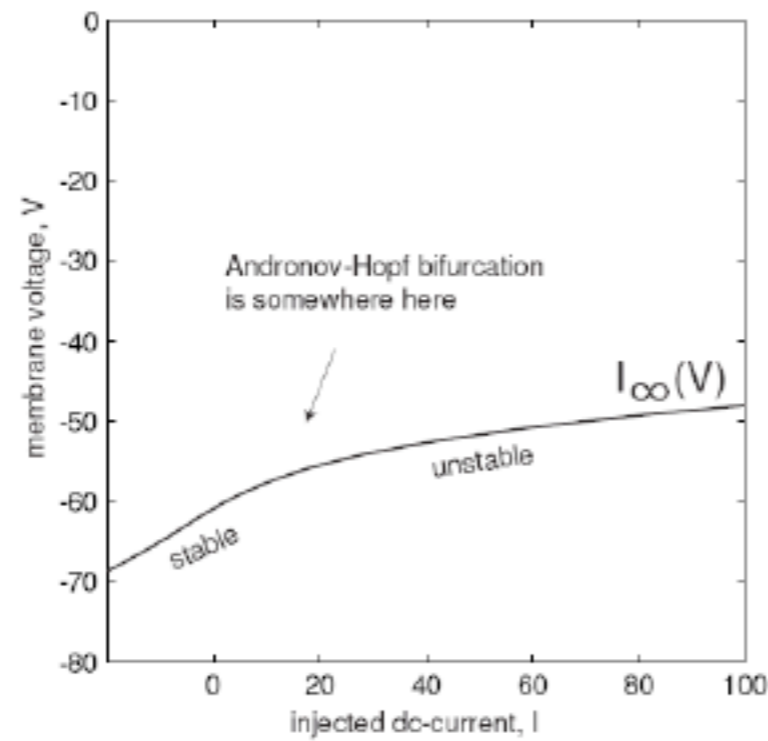
# Two-dimensional neural models

- Supercritical Hopf bifurcation in the  $I_{na,p} + I_K$  model with low-threshold  $K^+$  current when  $I=12$

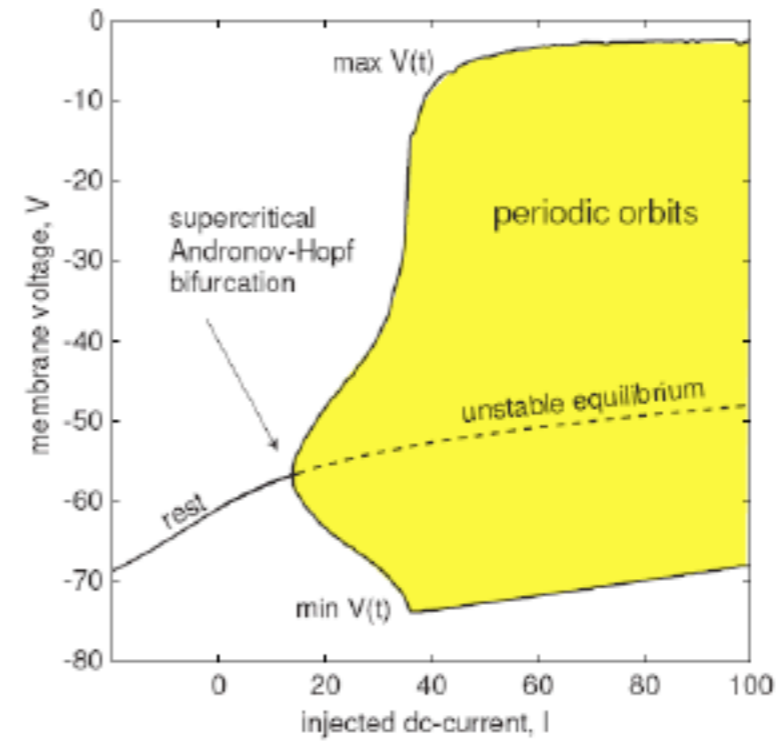


# Two-dimensional neural models

- Supercritical Hopf bifurcation in the  $I_{na,p} + I_K$  model with low-threshold  $K^+$  current when  $I=12$



a

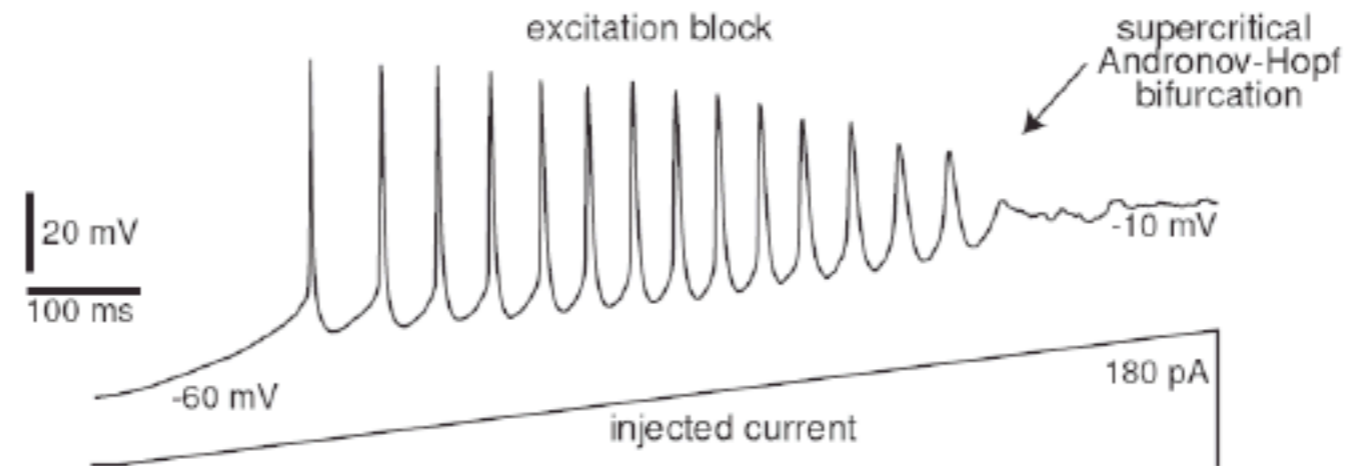


b



# Two-dimensional neural models

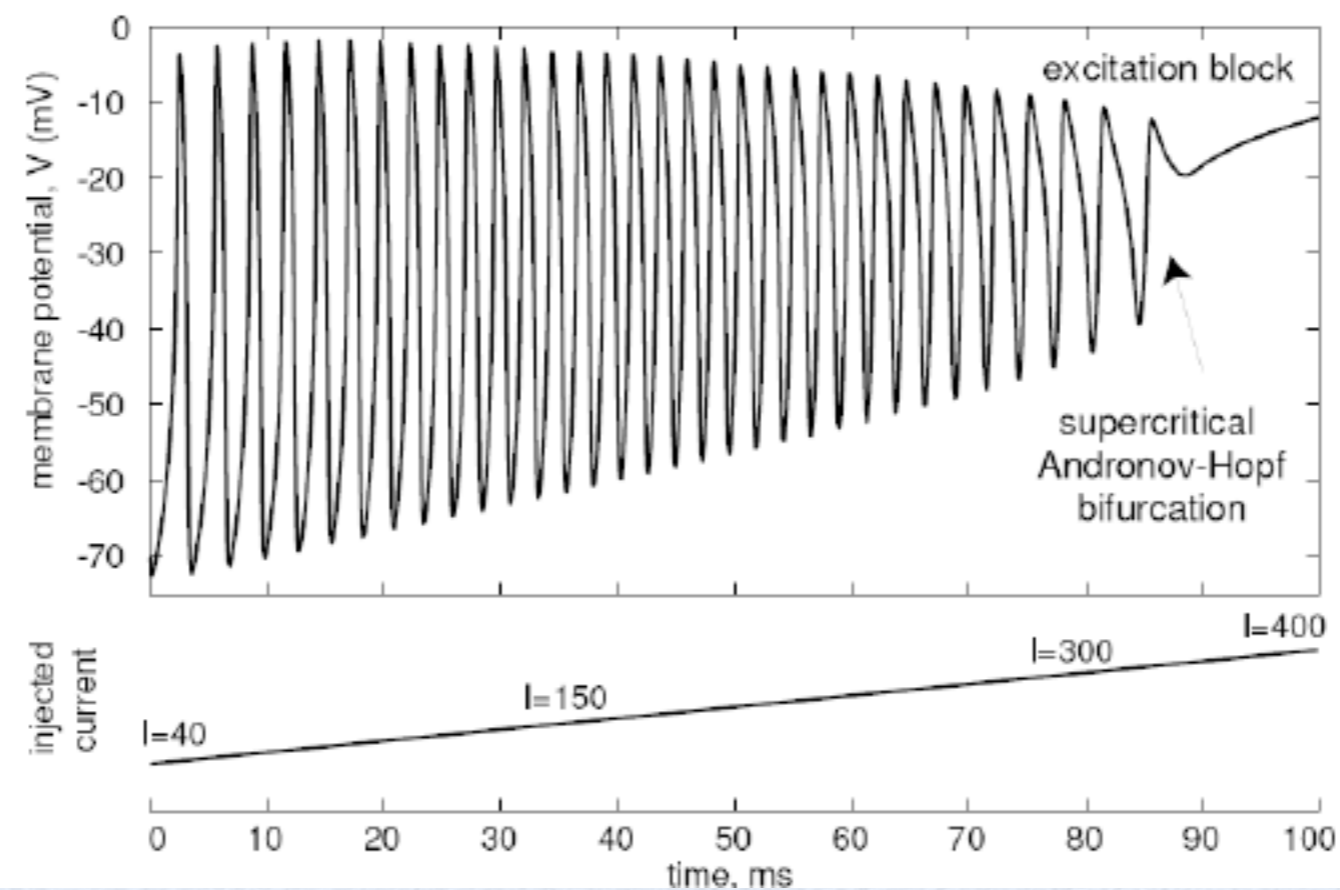
## □ Supercritical Hopf bifurcation



Excitation block in layer 5 pyramidal neuron of rat's visual cortex as the amplitude of the injected current ramps up

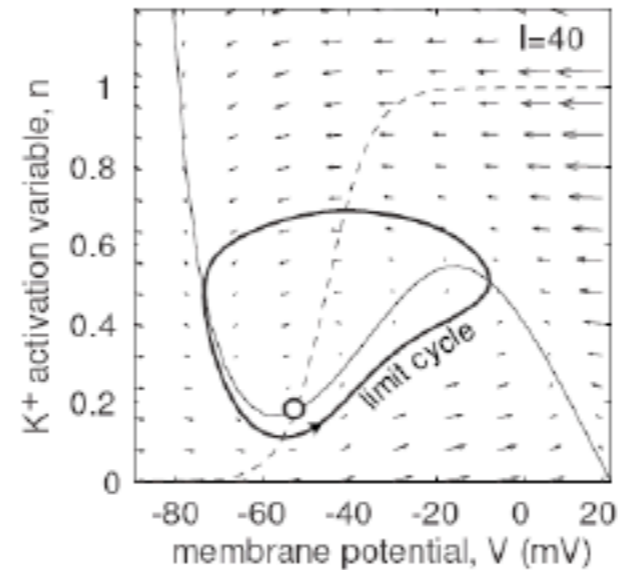
# Two-dimensional neural models

## □ Supercritical Hopf bifurcation in the $I_{na,p} + I_K$ model



# Two-dimensional neural models

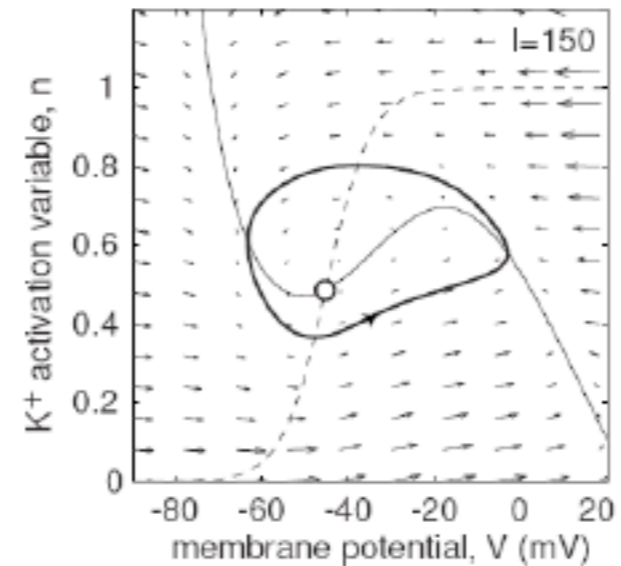
- Supercritical Hopf bifurcation in the  $I_{Na,p} + I_K$  model



Excitation block in the  $I_{Na,p} + I_K$ -model: As the magnitude of the injected current  $I$  ramps up, the spiking stops

# Two-dimensional neural models

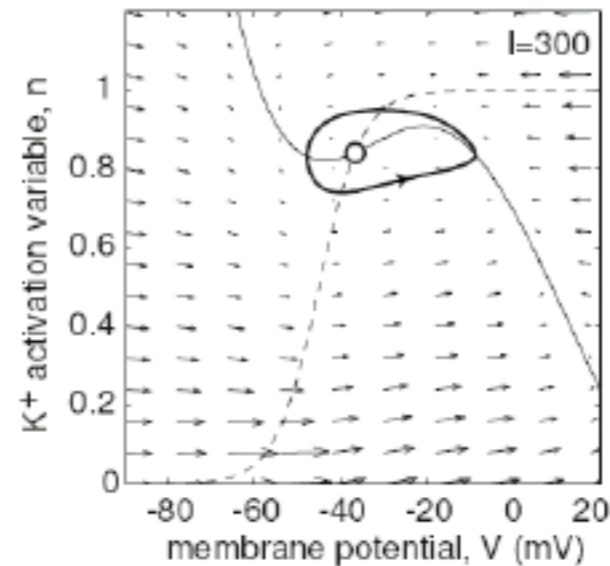
- Supercritical Hopf bifurcation in the  $I_{Na,p} + I_K$  model



Excitation block in the  $I_{Na,p} + I_K$ -model: As the magnitude of the injected current  $I$  ramps up, the spiking stops

# Two-dimensional neural models

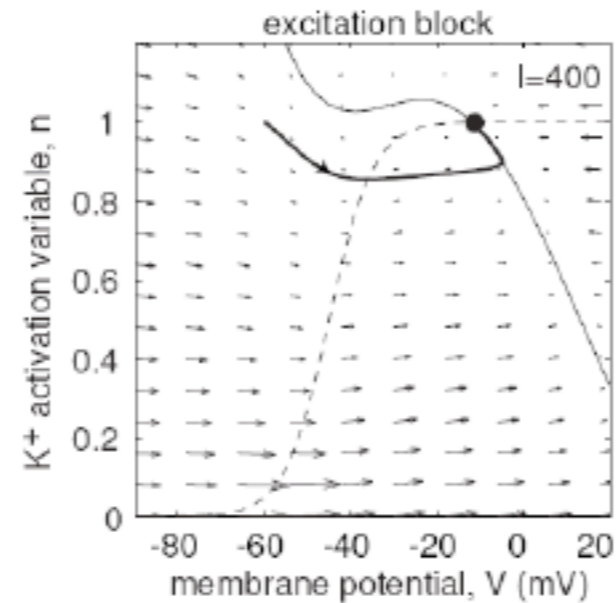
- Supercritical Hopf bifurcation in the  $I_{Na,p} + I_K$  model



Excitation block in the  $I_{Na,p} + I_K$ -model: As the magnitude of the injected current  $I$  ramps up, the spiking stops

# Two-dimensional neural models

- Supercritical Hopf bifurcation in the  $I_{Na,p} + I_K$  model



Excitation block in the  $I_{Na,p} + I_K$ -model: As the magnitude of the injected current  $I$  ramps up, the spiking stops

Aug24-11